Developmental Biology 335 (2009) 340–355

Contents lists available at ScienceDirect

Developmental Biology

journal homepage: www.elsevier.com/developmentalbiology

Characterization of the *Caenorhabditis elegans* UDP-galactopyranose mutase homolog *glf-1* reveals an essential role for galactofuranose metabolism in nematode surface coat synthesis

Jacopo F. Novelli [a], Kshitiz Chaudhary [a], Julie Canovas [a], Jack S. Benner [a], Catherine L. Madinger [a], Paul Kelly [c], Jonathan Hodgkin [b], Clotilde K.S. Carlow [a,*]

[a] *Division of Molecular Parasitology, New England Biolabs, Inc., 240 County Road, Ipswich, MA 01938, USA*
[b] *Department of Biochemistry, Genetics Unit, South Parks Road, OX1 3QU Oxford, UK*
[c] *Salem State College, 352 Lafayette Street, Salem, MA 01970, USA*

ARTICLE INFO

Article history:
Received for publication 30 March 2009
Revised 15 August 2009
Accepted 7 September 2009
Available online 12 September 2009

Keywords:
C. elegans
Galactofuranose
UGM
Surface coat
Glycans
M. nematophilum
Nematodes

ABSTRACT

Galactofuranose (Gal_f), the furanoic form of D-galactose produced by UDP-galactopyranose mutases (UGMs), is present in surface glycans of some prokaryotes and lower eukaryotes. Absence of the Gal_f biosynthetic pathway in vertebrates and its importance in several pathogens make UGMs attractive drug targets. Since the existence of Gal_f in nematodes has not been established, we investigated the role of the *Caenorhabditis elegans* UGM homolog *glf-1* in worm development. *glf-1* mutants display significant late embryonic and larval lethality, and other phenotypes indicative of defective surface coat synthesis, the glycan-rich outermost layer of the nematode cuticle. The *glf* homolog from the protozoan *Leishmania major* partially complements *C. elegans glf-1*. *glf-1* mutants rescued by *L. major glf*, which behave as *glf-1* hypomorphs, display resistance to infection by *Microbacterium nematophilum*, a pathogen of rhabditid nematodes thought to bind to surface coat glycans. To confirm the presence of Gal_f in *C. elegans*, we analyzed *C. elegans* nucleotide sugar pools using online electrospray ionization–mass spectrometry (ESI-MS). UDP-Gal_f was detected in wild-type animals while absent in *glf-1* deletion mutants. Our data indicate that Gal_f likely has a pivotal role in maintenance of surface integrity in nematodes, supporting investigation of UGM as a drug target in parasitic species.

Introduction

Complex glycans play a key role in a number of distinct processes in living organisms, such as maintenance of structural integrity, protection, morphogenesis and host–pathogen interactions (reviewed by Varki, 1993). The free-living rhabditid nematode *Caenorhabditis elegans* is a well-established model organism used to investigate many aspects of metazoan biology. Recently there has been much interest in its glycosylation pathways. Studies in *C. elegans* as well as other nematodes have confirmed the extensive conservation in the glycomic repertoire among metazoans, and revealed that nematode glyco-conjugates also possess several distinctive features that set them apart from vertebrates as well as other metazoans. In parasitic nematodes, unique glycans have primarily been isolated as excretory/secretory (ES) products and surface coat components.

Nematodes are encased in a multilayered collagenous cuticle, synthesized by the underlying hypodermal cells, that is shed periodically at molts (for a recent review, see Page and Johnstone, 2007). The outermost layer of the cuticle, referred to as the surface coat or glycocalyx, has a distinct composition, being made of loosely bound glyco-conjugates produced by the hypodermis and specialized pharyngeal secretory glands (for a review on the nature of nematode surface coat, see Bird and Bird, 1991). The main function of the glycocalyx is to act as a first line of defense from the external environment; in parasitic nematodes, the glycocalyx has also been implicated in immune evasion, immuno-suppression and immuno-modulation. Highly immunogenic mucin-type glycoproteins containing unusual *O*-methylated fucose (Fuc) and galactose (Gal) residues have been identified in the ES products of animal parasitic nematodes of the *Toxocara* genus (Khoo et al., 1991; Page et al., 1992). Indeed the immunogenicity of *Toxocara canis* in the mammalian host is mediated by these methylated residues (Schabussova et al., 2007). It is widely accepted that the *Toxocara* surface coat acts as a decoying device, diverting the immune attack to a labile structure which is continuously shed, thus allowing the worm to escape unscathed (Blaxter et al., 1992). *C. elegans* also methylates its mucin-type *O*-glycans (Guerardel et al., 2001), which display some additional atypical features such as the presence of glucose (Glc) and of trisubstituted *N*-acetylgalactosaminol

* Corresponding author. Fax: +1 978 921 1350.
E-mail address: carlow@neb.com (C.K.S. Carlow).

0012-1606/$ – see front matter © 2009 Elsevier Inc. All rights reserved.
doi:10.1016/j.ydbio.2009.09.010

(GalNAc) moieties (Guerardel et al., 2001). Nematode N-glycans are subject to esterification with phosphorylcholine; this modification, which also occurs in *C. elegans* (Cipollo et al., 2002), is considered one of the key mediators of the immunomodulatory and immunosuppressant activities displayed by secreted glycoproteins of filarial nematodes (Harnett and Harnett, 2001; Maizels et al., 1987). The parasitic nematode *Trichinella spiralis*, the causative agent of trichinellosis, secretes surface glycoproteins containing the sugar 3,6-dideoxy-D-arabino-hexose, or tyvelose (Wisnewski et al., 1993), a constituent of bacterial cell wall lipopolysaccharide (LPS). This sugar, which has never been reported in any other eukaryotic organism, appears to play a crucial role in infection, as shown by the observation that anti-tyvelose monoclonal antibodies are sufficient to efficiently block larval invasion of tissue cultured mammalian cells (McVay et al., 1998). In addition, the tyvelose-containing glycoproteins may also be involved in cell reprogramming and maintenance of the intracellular niche in the host (Despommier et al., 1990). These findings emphasize the importance of further investigation into the unique features of nematode glycan synthesis. Such studies will improve our understanding of nematode biology and may uncover some fundamental processes crucial for establishment and maintenance of the infection by parasitic species, and this in turn may lead to the development of novel methods of control (for a review on immunogenic glyco-conjugates of parasitic nematodes, see Dell et al., 1999). In this study, we describe yet another unusual feature of the nematode glycome, namely, the occurrence of galactofuranose (Gal_f) synthesis.

Galactopyranose (Gal_p), which is the thermodynamically favored pyranoic form of D-Gal, is ubiquitously found across species. In contrast, the furanoic form Gal_f has a more sporadic distribution and has only been identified in some microorganisms, namely, prokaryotes, protozoa and fungi (for a recent review, see Pedersen and Turco, 2003). Gal_f residues are components of cell wall glyco-conjugates of several bacterial pathogens: it has been identified in the galactan of *Mycoplasma mycoides* (Plackett and Buttery, 1964), the T1 antigen of *Salmonella* spp. (Sarvas and Nikaido, 1971) and the LPS *O*-antigen of *Escherichia coli* (Nassau et al., 1996) and *Klebsiella pneumoniae* (Koplin et al., 1997). Furthermore, Gal_f is a component of the cell wall arabinogalactan of *Mycobacteria* (Pan et al., 2001; Weston et al., 1997), including the causative agents of tuberculosis and leprosy. Gal_f is also found in several eukaryotic pathogens, including the protozoans *Leishmania* spp., the etiological agent of Leishmaniasis, and *Trypanosoma cruzi*, which is responsible

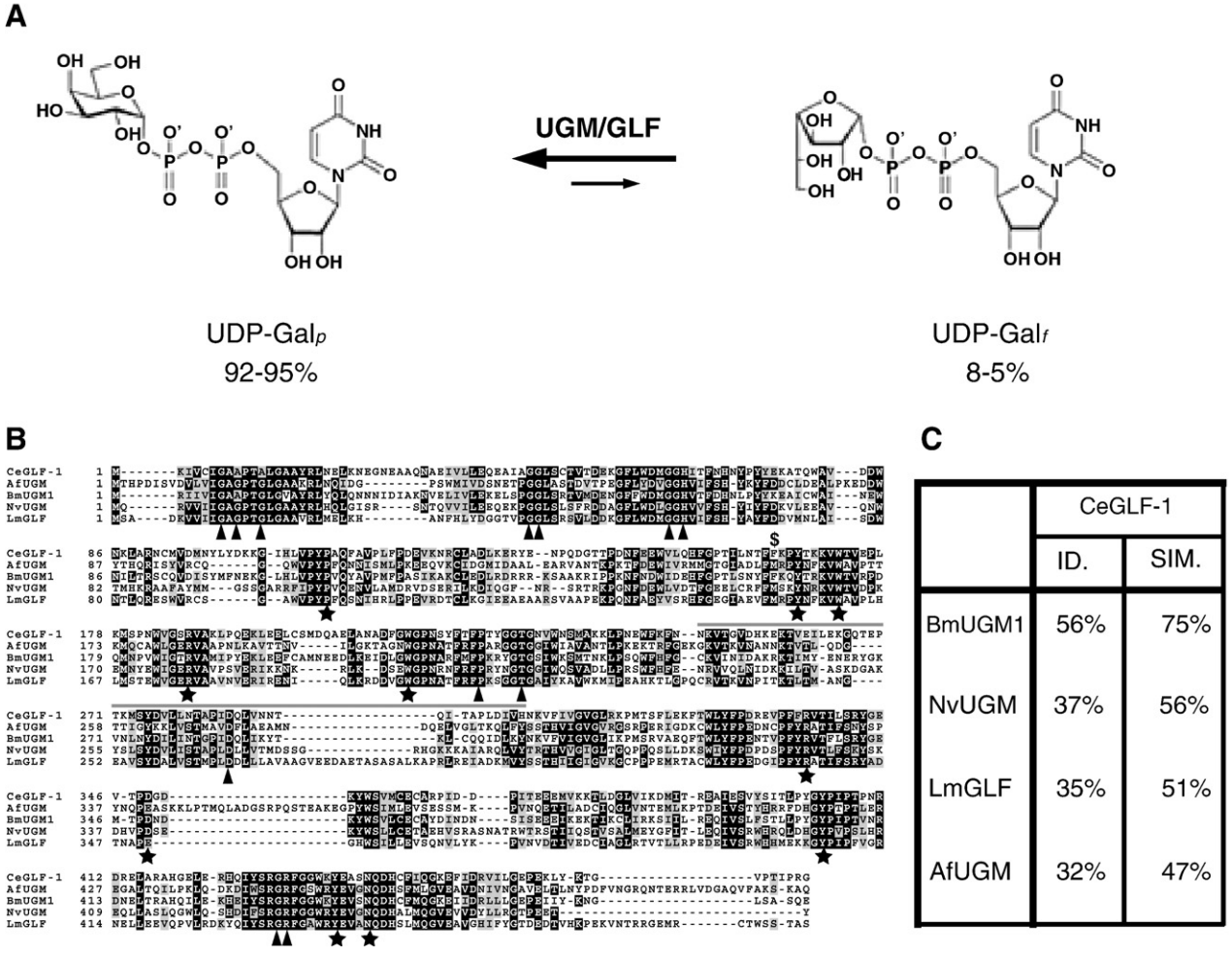

Fig. 1. Reaction catalyzed by UGMs and sequence analysis of some eukaryotic UGM homologs. (A) UGM/GLF catalyzes the interconversion between UDP-Gal_p and UDP-Gal_f, with equilibrium constants heavily skewed towards production of the pyranose form. (B) Alignment of amino acid sequences of *B. malayi* UGM (BmUGM1; Genbank accession # bankit1201054 FJ860969), *C. elegans* GLF-1 (CeGLF-1; NCBI accession # NP_500884), *Nematostella vectensis* UGM homolog (NvUGM; NCBI accession # XP_001624068), *L. major* GLF (LmGLF; NCBI accession # XP_001682426) and *A. fumigatus* UGM (AfUGM; NCBI accession # CAI38754.2). Alignment was performed using the TCOFFEE alignment software (http://tcoffee.vital-it.ch/cgi-bin/Tcoffee/tcoffee_cgi/index.cgi) (Poirot et al., 2003) and colored using BOXSHADE (http://www.ch.embnet.org/software/BOX_form.html). The positions of the active site conserved residues are indicated by a star, while the residues involved in FAD binding (as identified by Chad et al., 2007) are marked by a triangle. The location of the stop codon introduced by the *tm2621* deletion is indicated by a dollar sign. The extent of the in-frame *tm2412* deletion is marked by a grey bar. (C) Overall percentage amino acid identity (ID.) and similarity (SIM.) of CeGLF-1 to the four eukaryotic UGM homologs reported in the alignment.

for Chagas disease. In these organisms, Gal_f residues are incorporated into various glyco-conjugates, namely, lipophosphoglycan and glycoinositolphospholipids in *Leishmania* spp. (Ilg et al., 1992; McConville et al., 1990; Turco et al., 1989), and mucins, glycosylphosphoinositol-anchored proteins and lipids in *T. cruzi* (De Arruda et al., 1989; de Lederkremer and Colli, 1995; Previato et al., 1990), which collectively constitute the bulk of the protozoan surface coat. The *Leishmania* surface coat glyco-conjugates play an important role in infection and protection from hydrolytic enzymes, oxidants and the human complement (Spath et al., 2003). Exposure to anti-Gal_f antibodies impairs invasion of host cells by *T. cruzi*, suggesting a role in infection for Gal_f-containing glyco-conjugates (De Arruda et al., 1989). Gal_f residues are also found in the cell wall glycans of fungi, such as *Aspergillus* spp. (Hearn et al., 1989; Wallis et al., 2001) and *Cryptococcus neoformans* (James and Cherniak, 1992). Some of these fungal species constitute a serious and often lethal threat for immuno-compromised individuals (reviewed by Nielsen and Heitman, 2007).

The only biosynthetic route to Gal_f synthesis is the conversion of the nucleotide sugar (NS) precursor UDP-Gal_p into UDP-Gal_f, which is catalyzed by the enzyme UDP-galactopyranose mutase [UGM, Enzyme Commission (E.C.) number 5.4.99.9] (Fig. 1A). Bacterial UGMs are encoded by *glf* loci (galactofuranose synthesis); confusingly, in the literature the acronym GLF is sometimes also applied to the gene product. Bacterial UGM/GLFs are flavin adenine dinucleotide (FAD)-dependent coenzymes with a molecular weight of approximately 40 kDa. The prokaryotic enzymes are well characterized, and high-resolution crystal structures of the *K. pneumoniae*, *Mycobacterium tuberculosis* and *E. coli* enzymes have been obtained (Beis et al., 2005; Sanders et al., 2001).

The *Mycobacterium smegmatis glf* locus is essential for viability: knockout mutants fail to grow upon loss of the rescuing plasmid, carrying functional copies of the *M. tuberculosis glf* open reading frame (ORF) (Pan et al., 2001); the lethality is attributed to failed bacterial cell wall synthesis in the absence of Gal_f. In *E. coli*, the *glf* locus is required for synthesis of the LPS *O*-antigen, but dispensable for viability (Koplin et al., 1997).

Eukaryotic UGMs share only 25–30% identity with their bacterial counterparts; however, most residues required for substrate or FAD binding are conserved (Beverley et al., 2005). *Leishmania major glf* knockouts are both viable and infectious but display decreased virulence in a mouse model (Kleczka et al., 2007). *glf* knockouts have been recently generated or recovered for three *Aspergillus* species: *A. fumigatus*, *A. niger* and *A. nidulans* (Damveld et al., 2008; El-Ganiny et al., 2008; Schmalhorst et al., 2008). In all three cases, loss of Gal_f synthesis is compatible with viability but results in a reduction in cell wall thickness, which in turn is accompanied by defective morphogenesis, hypersensitivity to drugs and osmotic stress. Significantly, deletion of *glf* in *A. fumigatus* results in attenuated virulence in a mouse model (Schmalhorst et al., 2008), as observed for *L. major glf* loss-of-function mutants.

The presence of UGM in several prokaryotic and eukaryotic microbial pathogens, the important roles played by Gal_f-containing glycans in these organisms and the absence of the biosynthetic pathway in higher eukaryotes have led to the proposal of Gal_f metabolism as a target for broad-spectrum chemotherapeutic intervention (reviewed by Pedersen and Turco, 2003). A microtiter plate assay for the *M. tuberculosis* UGM has been developed and used to screen a compound library (Scherman et al., 2003). Likewise, a fluorescence polarization-based high-throughput assay for the *K. pneumoniae* UGM has been devised and used for library screening (Carlson et al., 2006; Soltero-Higgin et al., 2004). Other groups have reported the synthesis of various substrate analogs, and have demonstrated their inhibitory activity on UGMs from different bacterial species (Desvergnes et al., 2007; Dykhuizen et al., 2008; Ghavami et al., 2004; Itoh et al., 2007; Veerapen et al., 2004), holding promise for the development of broad-spectrum compounds which are also active against eukaryotic UGMs.

The existence of Gal_f metabolism in nematodes has remained uncertain. The genome and EST sequencing projects indicate the presence of genes encoding UGM homologs in most nematode clades, suggesting that synthesis of Gal_f is an ancient and conserved feature of the phylum (Beverley et al., 2005). Significantly, the *C. elegans glf-1* ORF, encoding the sole UGM homolog in this species, functions in *E. coli* in an *in vivo* complementation assay for UDP-Gal_f synthesis (Beverley et al., 2005). Genome-wide RNA interference (RNAi) screens in *C. elegans* suggested that downregulation of *glf-1* is detrimental (Ashrafi et al., 2003; Kamath et al., 2003; Rual et al., 2004; Samuelson et al., 2007; Simmer et al., 2003). However, a detailed characterization of the *C. elegans glf-1* gene function has not been performed and, most importantly, Gal_f has never been isolated from any nematode species, leaving the question open as to whether the Gal_f pathway is functional in the phylum and what developmental role, if any, is performed by Gal_f residues in nematodes.

In this study we have carried out a detailed genetic and molecular analysis of the *C. elegans glf-1* locus. Our data demonstrate that Gal_f synthesis occurs in *C. elegans*, and we provide evidence that Gal_f is required for maintenance of the integrity of surface coat. Our results demonstrate that this structure has a role in completion of embryogenesis, late larval development and survival of the nematode in an adverse environment.

Materials and methods

Strains and genetic methods

N2 strain var. Bristol was used as wild-type (WT) (Brenner, 1974). Animals were cultured at 20 °C according to standard methods (Sulston and Hodgkin, 1988).

The following mutant strains were used:

TM2412 *glf-1(tm2412) IV*
TM2621 *glf-1(tm2621) IV*
RB1032 *osr-1(ok959) I*
HT1593 *unc-119(ed3) III*

Strains were obtained from the *C. elegans* stock center (CGC, University of Minnesota) and from Dr. S. Mitani (National Bioresource Project of Japan, Tokyo Women's Medical University School of Medicine, Tokyo).

The following transgenic strains were generated and used in this work:

IP604 *glf-1(tm2412): nbEx146[pTG96; glf-1p::Ceglf-1::3′UTR]*
IP605 *glf-1(tm2412): nbEx147[pTG96; glf-1p::Ceglf-1::3′UTR]*
IP609 *glf-1(tm2621): nbEx146[pTG96; glf-1p::Ceglf-1::3′UTR]*
IP612 *glf-1(tm2412): nbEx153[pTG96; glf-1p::Ceglf-1cDNA::3′UTR]*
IP613 *glf-1(tm2412): nbEx154[pTG96; glf-1p::Ceglf-1cDNA::3′UTR]*
IP614 *glf-1(tm2412): nbEx155[pTG96; glf-1p::Lmglf::3′UTR]*
IP615 *glf-1(tm2412): nbEx156[pTG96; glf-1p::Lmglf::3′UTR]*
IP616 *glf-1(tm2412): nbEx157[pTG96; glf-1p::Lmglf::3′UTR]*
IP617 *glf-1(tm2412): nbEx158[pTG96; glf-1p::Lmglf::3′UTR]*
IP620 *glf-1(tm2412); osr-1(ok959): nbEx161[pTG96; gale-1p::Ceglf-1::3′UTR]*
IP621 *glf-1(tm2412); osr-1(ok959): nbEx162[pTG96; gale-1p::Ceglf-1::3′UTR]*
IP623 *glf-1(tm2412); osr-1(ok959): nbEx164[glf-1p::Ceglf-1::GFP]*
IP624 *glf-1(tm2412); osr-1(ok959): nbEx165[glf-1p::Ceglf-1::GFP]*
IP625 *glf-1(tm2412); osr-1(ok959): nbEx166[glf-1p::Ceglf-1::GFP]*
IP629 *glf-1(tm2412); nbEx169[sur-5p::Ceglf-1::GFP]*
IP630 *glf-1(tm2412); osr-1(ok959): nbEx170 [sur-5p::Ceglf-1::GFP]*
IP638 *unc-119(ed3); nbEx170 [pDP#MM016b; sur-5p::Ceglf-1::GFP]*

RNA interference (RNAi)

RNAi of *glf-1* (gene H04M03.4) and *gale-1* (gene C47B2.6) was performed by microinjection of double stranded RNA (dsRNA) corresponding to exons and intervening sequences of the gene of interest. For *glf-1*, the PCR product used as a template for dsRNA synthesis corresponds to the portion of the *glf-1* gene between exons 3 and 6. For *gale-1*, the amplicon spanned exon 4 and part of exon 5. In both cases, genomic fragments were amplified from *C. elegans* genomic DNA preparations. dsRNA was synthesized using the Highscribe Kit (New England Biolabs, NEB) according to the manufacturer's guidelines and delivered by injection as previously described (Fire et al., 1998). Combinatorial RNAi of *glf-1* and *gale-1* was performed by mixing the two dsRNAs in a 1:1 ratio and injecting the mixture. A list of primers used for the amplification of the fragments can be found in Supplementary Table 1.

Lectin staining, protease sensitivity, alkaline hypochlorite sensitivity and permeability assays

WGA (wheat germ agglutinin), SBA (soy bean agglutinin), ConA (Concanavalin A), PNA-fluorescein isothiocyanate (FITC) (peanut agglutinin), UEA-1 (*Ulex europaeus* agglutinin) and PSA (*Pisum sativum* agglutinin), all conjugated to FITC, were purchased from Biomeda. Generally, staining and destaining were performed as previously described (Gravato-Nobre et al., 2005). In the case of UEA-1 and WGA, staining was performed without the addition of Triton X-100 in the staining buffer, since the detergent solubilized completely the reactive sugars. Alkaline hypochlorite sensitivity tests were also carried out as previously described (Gravato-Nobre et al., 2005). Thirty individual animals were tested per each strain. *glf-1* mutants die immediately when placed in a bleach solution, precluding accurate measurement of the time taken to stop thrashing. Hence, only the time taken for the first break to appear was recorded. Collected data were subjected to statistical analysis using the Prism 4 program (GraphPad Software, Inc., La Jolla, CA). One-way ANOVA with Dunnet post hoc comparisons were performed. A P value of less than 0.05 was considered statistically significant. Transgenic strains, carrying an extrachromosomal array, were individually inspected for somatic mosaicisms using the *sur-5::GFP* co-injection marker (Yochem et al., 1998) or, in the case of IP623-IP624-IP625, the *glf-1::gfp* marker was used. Only worms that did not display somatic mosaicism were employed in the test. Protease sensitivity assays were performed by placing 100 young living hermaphrodites into a watchglass containing a 3 mM $CaCl_2$ solution. Proteinase K (NEB) was then added at a final concentration of 2 mg/ml. After incubation for 1 h at room temperature, the number of enzymatically digested worms was counted. Hoechst 33258 staining (Sigma-Aldrich, St. Louis, MO) was performed as described (Moribe et al., 2004).

Production of constructs and transgenes

Standard molecular biology techniques were used (Sambrook et al., 1989). Amplification steps for construct generation described below were carried out using Phusion DNA polymerase (NEB) or Taq polymerase (NEB).

The *glf-1p::Ceglf-1::3′UTR* genomic rescue construct was generated by amplifying from N2 genomic DNA a 8054 bp fragment including 2195 bp of the *glf-1* 5′ region, the full 3739 bp genomic sequence (gene H04M03.4) and 2120 bp of the *glf-1* 3′ untranslated region (UTR). This amplicon includes the flanking sequences between *glf-1* and the upstream and downstream ORFs (H04M03.11 and H04M03.3, respectively). The resulting DNA fragment was cloned in TOPO TA pCR 2.1 (Invitrogen) according to the manufacturer's instructions.

glf-1p::Ceglf-1::GFP, encoding a GLF-1::GFP fusion driven by the *glf-1* endogenous promoter, was generated by amplifying from *glf-1p::Ceglf-1::3′UTR* a 5931 bp genomic fragment including the aforementioned *glf-1* 5′ sequence and the full genomic sequence upstream of the termination codon. The resulting PCR product was cloned in frame with the *gfp* sequence into vector pPD95.75 (a gift from A. Fire, Stanford University, Stanford, CA).

glf-1p::Ceglf-1cDNA::3′UTR was generated in two steps by replacing the C-terminal GFP fusion of *glf-1p::Ceglf-1::GFP* with 1965 bp of the *glf-1* 3′UTR preceded by a termination codon and subsequently by swapping the genomic *glf-1* sequence with the *glf-1* cDNA sequence. The *glf-1* cDNA was amplified with gene specific primers from N2 *C. elegans* cDNA pools (a kind gift of Yinhua Zhang, NEB, MA).

glf-1p::Lmglf::3′UTR was generated as described for *glf-1p::Ceglf-1cDNA::3′UTR*, except that the *L. major* gene was inserted between the *glf-1* promoter and 3′UTR. The intronless *L. major glf* gene (Bakker et al., 2005) was amplified with gene specific primers from *L. major* strain *Friedlin* genomic DNA preparations. Likewise *glf-1p::Ecglf::3′UTR* was generated by inserting the K-12 *E. coli glf* locus (Stevenson et al., 1994) between *glf-1* 5′ and 3′ UTR.

gale-1p::Ceglf-1::3′UTR translational fusion was generated by replacing the *glf-1* promoter in construct *glf-1p::Ceglf-1::3′UTR* with 2693 bp of *gale-1* promoter sequence upstream of the initiation codon.

sur-5p::Ceglf-1::GFP was generated by replacing the *glf-1* promoter in construct *glf-1p::Ceglf-1::GFP* with 3.5 kb of the 5′ sequence of *sur-5* upstream of the ATG contained in plasmid pTG96 (Yochem et al., 1998).

All constructs were verified by multiple restriction digests and DNA sequencing of both strands prior to injection. A list of primers used can be found in Supplementary Table 1.

Constructs were injected into *glf-1(tm2412)* worms, *glf-1 (tm2142); osr-1(ok959)* double mutants or *unc-119(ed3)* worms according to standard protocols (Mello et al., 1991). In most cases, plasmid pTG96, carrying a *sur-5::GFP* reporter (Yochem et al., 1998), was included as a co-injection marker. Plasmid pDP#MM016b, carrying a *unc-119(+)* rescue construct (Maduro and Pilgrim, 1995), was used in generation of the transgenic strain IP638. Injection mixtures had the following composition: plasmid of interest 10–30 ng/μl; co-injection marker 10–30 ng/μl; low weight molecular marker (NEB) as a filler to a final 100 ng/μl concentration. For each construct, at least two independent transgenic lines were established and inspected.

Microscopy

Live samples for microscopy were prepared according to standard protocols (Sulston and Hodgkin, 1988). DIC micrographs were acquired with a Zeiss Axiovert 200MT (Zeiss, Munich, Germany) equipped with epifluorescence and processed using the Axiovision package release 4.5. Confocal pictures were acquired with a LSM 510 META laser scanning microscope (Zeiss) and processed with the LSM Zeiss package release 4.2. Scanning electron microscopy (SEM) specimens were fixed in 2.5% glutaraldehyde in phosphate buffer, pH 7.4, dehydrated in an ethanol series (0% to 100% in 10% increments, 10 min each) and critical-point dried. Specimens were coated with approximately 20 nm of a 60/40 gold/palladium alloy in a Sputter coater (Fisons), mounted, and observed on a 6360-LV Scanning Electron Microscope (JEOL).

Infection of C. elegans with Microbacterium nematophilum

Challenge of *C. elegans* with *Microbacterium nematophilum* and SYTO 13 (Invitrogen) staining of infected worms was carried out according to standard protocols (Hodgkin et al., 2000).

NS analysis

For extraction of *C. elegans* NSs, we adapted the protocol described by Turnock and Ferguson (2007), which was originally devised for purification of NSs from the protozoans *Trypanosoma* spp. and *L. major*. Commercially available NS standards UDP-Glc, UDP-GlcNac, UDP-Gal_p, GDP-Man, GDP-Fuc and GDP-Glc were purchased from Sigma-Aldrich. UDP-Gal_f was a kind gift of Dr. Michael McNeil. NS extracts were prepared from 2 ml pellets of live worms. Worms were washed extensively in M9 buffer (Sulston and Hodgkin, 1988) and incubated at room temperature in M9 buffer for 3 h to allow complete digestion of bacteria in the gut. To monitor the reproducibility of the results, the pool of worms was divided into two equal samples and processed in parallel. Worms were gently sonicated until approximately 90% disruption was obtained. The lysate was then centrifuged at 14,000 × *g* for 15 min at 4 °C and the supernatant was extracted three times with 400 µl of 90% butan-1-ol (v/v) to remove lipids. The resulting aqueous phase was dried to completion and resuspended in 1 ml of 10 mM ammonium bicarbonate. NSs were separated with a Supelco Envi-Carb graphitized carbon solid phase extraction cartridge (1 ml/100 mg; Sigma) as previously described (Rabina et al., 2001). The elutant from the graphitized carbon cartridge was applied to a Develosil RP-Aqueous-3 (1 mm × 150 mm) column (Nomura Chemical Company) equilibrated at 50 mM triethylammonium acetate (TEAA), pH 6.0, at a flow rate of 75 µl/min, and developed with a gradient of 0–8% acetonitrile over 14 min. The effluent from this column was analyzed online by an Agilent 6120 time-of-flight (TOF)

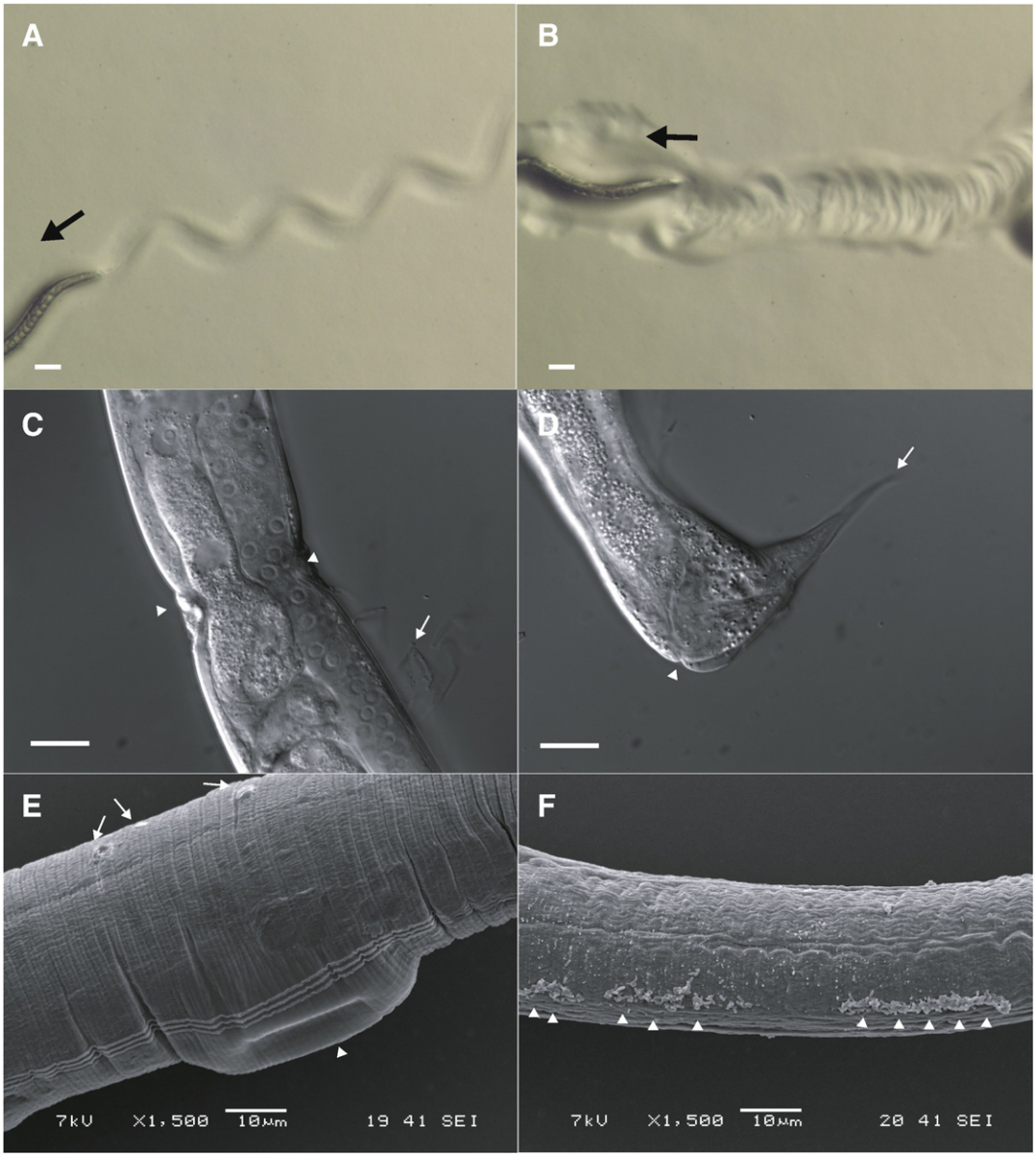

Fig. 2. Visible phenotypes expressed by *glf-1(RNAi, tm2412, tm2621)* worms. (A) and (B) are micrographs taken directly from *C. elegans* growth plates seeded with *E. coli*. (C) and (D) are DIC micrographs, while (E) and (F) are scanning electron micrographs. (A and B) Skd phenotype typical of *glf-1* mutants. The black arrows mark the direction of the worms' movement. While a WT worm leaves a regular sinusoidal trail on the *E. coli* lawn (A) a *glf-1* mutant leaves a broader and irregular track in its wake (B) due to the lack of traction. (C) Body constriction phenotype. Arrowheads point to the pinched area of the cuticle. Note also the surface layer sloughing off (white arrow), characteristic of *glf-1* mutants. (D) Distortion of the anal region in a *glf-1* mutant. The white arrowhead marks the position of the anus, while the arrow points to the tip of the tail. (E) Superficial blisters (arrows). Note also the ventral bulge (arrowhead), commonly observed in these mutants. (F) Adherence of *E. coli* cells (arrowheads) on the surface of a *glf-1* mutant. Scale bars, 100 µm (A and B), 20 µm (C and D) and 10 µm (E and F).

mass spectrometer with a capillary electrospray ionization source (Agilent Technologies) in negative ion mode with a capillary voltage of 3500 V from m/z 250 to 1650. Spectra were collected and analyzed with Analyst 1.1 software (Perkin Elmer). NSs were detected by ion extraction, by retention time and comparison of these Extracted Ion Chromatographs (EICs) to the EICs generated by the NS standards.

Semi-quantitative PCR

RNA was extracted using the RNeasy Kit (QIAGEN), quantified, treated with DNase I (NEB) and retrotranscribed using the Proscript II RT-PCR kit (NEB) according to the manufacturers' instructions. Semi-quantitative PCR was performed using a DyNAmo™ SYBR® Green qPCR Kit (NEB) in a MyIQ thermocycler (Bio-Rad, Hercules,

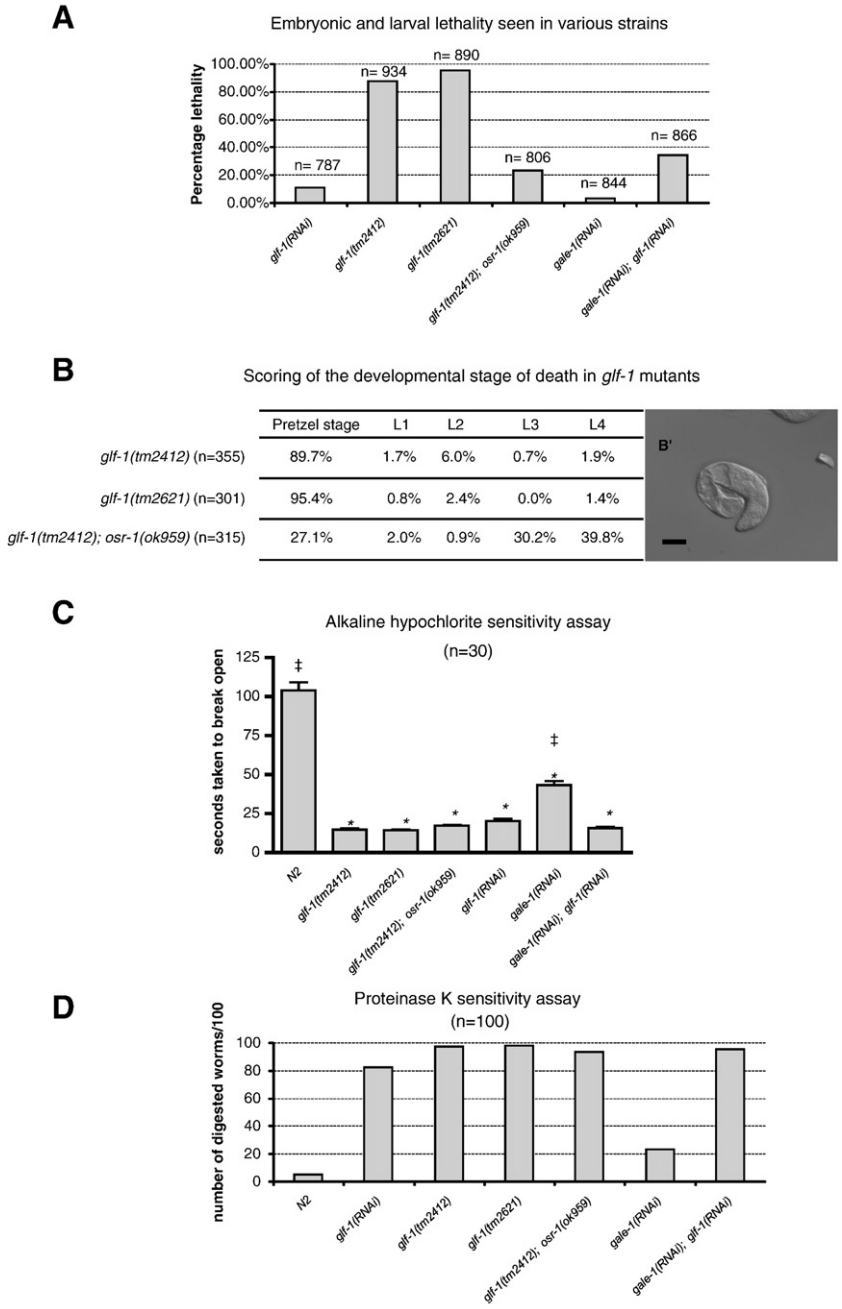

Fig. 3. Lethality and cuticle fragility tests. (A) Percentage of overall lethality exhibited by *glf-1(RNAi,tm2412,tm2621)* animals, *glf-1(tm2412); osr-1(ok959)* double mutants, *gale-1 (RNAi)* and *glf-1(RNAi)*; *gale-1(RNAi)* worms. Embryonic (Emb) larval (Lvl) lethality were combined in this test; for each strain, at least 700 worms were counted. (B) Stage-specificity of the lethality exhibited by *glf-1(tm2412, tm2621)* and *glf-1(tm2412); osr-1(ok959)* mutants. For the animals which failed to survive, the stage at which death occurred was scored and shown. A least 300 animals were scored for each strain. Most *glf-1(tm2412,tm2621)* worms arrested at late embryogenesis between the pretzel stage and hatching, and failed to leave the eggshell, as shown in (B′). (C) Alkaline hypochlorite sensitivity assay using *glf-1(RNAi, tm2412, tm2621)* animals, *glf-1(tm2412); osr-1(ok959)* mutants, *gale-1 (RNAi)* animals and *glf-1(RNAi); gale-1(RNAi)* worms. The mean and standard error (SEM) values obtained from 30 individual worms are shown. The asterisk indicates those datasets significantly different from N2 in one-way ANOVA significance tests (in all cases $P<0.01$); the double dagger indicates datasets that are significantly different from *glf-1(tm2412)* in one-way ANOVA significance tests (in all cases $P<0.01$). (D) Proteinase K dissolution assay of *glf-1(RNAi, tm2412, tm2621)*, *glf-1(tm2412); osr-1(ok959)* double mutants, *gale-1 (RNAi)* animals and *glf-1(RNAi); gale-1(RNAi)* worms. The bar represents the number of enzymatically digested animals (in all cases, $n=100$). For the experiments listed above, data were collected as described in Materials and methods. Scale bar, 10 μm (3B′).

CA) according to the manufacturers' instructions. Expression of *glf-1* was compared to that of a portion of 18S RNA using specific primers. A list of primers used can be found in Supplementary Table 1.

Results

Phenotypic characterization of glf-1(RNAi) worms and glf-1 knockouts

An alignment of several eukaryotic UGM representatives, including *C. elegans* GLF-1, is shown in Fig. 1B. While eukaryotic UGMs share on average only 25–30% overall sequence identity with prokaryotic UGMs, conservation within eukaryotic UGMs is greater. The predicted sequences of *Brugia malayi* UGM (BmUGM1) and *C. elegans* GLF-1 (CeGLF-1) are more similar to each other than to any other UGMs, supporting their phylogenetic relatedness (Fig. 1C). In *C. elegans* GLF-1 and *Brugia* UGM1, all residues that have implicated in FAD binding or play a role in formation of the active site are conserved (Fig. 1B).

To characterize the *glf-1* function, we performed RNAi and examined two *glf-1* deletion alleles: *tm2412* and *tm2621*. A 370-bp deletion in *glf-1(tm2412)* removes the entire sequence of exon 4 as well as some flanking intronic sequences. This deletion, which maintains the correct frame, removes at least one key residue within a highly conserved motif involved in FAD binding (Fig. 1B). *glf-1 (tm2621)* worms have a 283 bp deletion which removes a portion of exon 3 and the following intron. This mutation causes the 5′ region of exon 3 to fuse with the remainder of intron 3, thus introducing of an in-frame TGA stop codon 15 bp downstream of the rejoined ends. Translation of the GLF-1(TM2621) protein would result in a 165 amino acid long peptide lacking most of the residues essential for catalysis as well as the C-terminal FAD binding motif (dollar sign, Fig. 1B).

Phenotypic inspection of *glf-1(tm2412, tm2621, RNAi)* worms revealed that *glf-1* is required for normal post-embryonic development. When compared to wild-type (WT) worms (Fig. 2A), *glf-1* mutant worms and RNAi phenocopies exhibited a fully penetrant traction defect when moving on a bacterial lawn or on the agar surface (Fig. 2B and Supplementary movies 1 and 2). This defect is referred to as the Skiddy (Skd) phenotype (Darby et al., 2007; Gravato-Nobre et al., 2005; Partridge et al., 2008; Yook and Hodgkin, 2007). *glf-1* worms also express several partially penetrant phenotypes, such as lethality (Fig. 3A), body constrictions (Fig. 2C), a swollen post-anal region (Fig. 2D) and superficial blisters (Fig. 2E). Loss of *glf-1* activity also causes an unusual change in outer surface properties whereby *E. coli* cells adhere to the worm cuticle (Fig. 2F). In addition, *glf-1* mutants displayed enhanced cuticle fragility and poor long-term survival on plates upon starvation, indicating a general impairment in fitness.

Consistently, all phenotypes were exacerbated in deletion mutants in comparison to RNAi phenocopies. For instance, the overall lethality is markedly accentuated, with 87.5% of *tm2412* homozygotes and 95% of *tm2621* homozygotes dying during development, either as embryos or as larvae ($n=934$ and $n=890$, respectively; Fig. 3A), in contrast to the marginal overall lethality exhibited by RNAi phenocopies (10.9%; $n=787$; Fig. 3A). We confirmed that all phenotypes displayed by *glf-1* deletion mutants were fully recessive and *tm2412* and *tm2621* failed to complement each other.

To characterize lethality further, we determined precisely the onset of lethality in the two *glf-1* deletion alleles: *tm2412* and *tm2621*. In both cases, lethality peaked in late embryos, between the pretzel stage and hatching (Figs. 3B and B′; 89.7% in *glf-1(tm2412)* worms, $n=355$, and 95.4% in *glf-1(tm2621)* animals, $n=301$). Lower levels of lethality were seen in L2 larvae, and later larval stages (Fig. 3B). The pattern of lethality observed was consistent between the two alleles, which together with the nature of the DNA lesions involved suggest that *tm2621* and *tm2412* are both strong loss-of-function alleles, closely approaching the null state for the gene.

The gross phenotypic analysis suggested that *glf-1* mutants have a defect in the synthesis of the surface coat. Mutants characterized by defective surface coat synthesis are often hypersensitive to alkaline hypochlorite treatment (Darby et al., 2007; Gravato-Nobre et al., 2005; Yook and Hodgkin, 2007). We performed the standard alkaline hypochlorite sensitivity test which revealed that *glf-1 (tm2412,tm2621)* mutants and *glf-1(RNAi)* phenocopies are approximately five-fold more sensitive to alkaline hypochlorite exposure than WTs (Fig. 3C). Likewise, *glf-1* worms show almost 20-fold increase in sensitivity to proteinase K treatment [WTs: 5%; *glf-(RNAi)*: 82%; *glf-1(tm2412)*: 97%, *glf-1(tm2621)*: 98%; in all cases $n=100$; Fig. 3D].

glf-1 mutants and RNAi phenocopies desiccate within seconds when removed from the growth media and appear somewhat shrunken in comparison to WTs. This phenotype is reminiscent of that observed when *C. elegans* is exposed to hyperosmotic environments (Solomon et al., 2004). Loss-of-function mutations in *osr-1* confer enhanced resistance to osmotic stresses (Solomon et al., 2004). Introduction of the *osr-1* deletion allele *ok959* into the *glf-1(tm2412)* background efficiently suppresses the Glf-1 lethality [87.5% overall lethality observed in *glf-1(tm2412)* worms versus 23% observed in *glf-1(tm2412); osr-1(ok959)* double mutants; $n=806$; Fig. 3A]. We followed in detail the stage specificity of the marginal lethality exhibited by *glf-1(tm2412); osr-1(ok959)* worms, which was rather evenly distributed across late embryogenesis, L3 and L4 larval stages (Fig 3B; $n=315$). Statistical analysis revealed that *glf-1(tm2412); osr-1(ok959)* double mutants are as sensitive to hypochlorite as *glf-1 (tm2412)* single mutants ($P>0.05$) (Fig. 3C). Sensitivity to proteinase K treatment was also very similar between the two strains (93% and 97%, respectively) (Fig. 3D). These data indicate that suppression of the lethality by *osr-1* is a result of improved resistance to osmotic stress rather than by restoration and/or replacement of the endogenous *glf-1* gene function.

In *C. elegans*, a standard approach to characterizing surface coat mutants involves the use of labeled lectins. Plant lectins which fail to bind the surface of WT *C. elegans* (Figs. 4A and A′) stain mutants with defective surface coat structures (Link et al., 1992; Silverman et al., 1997). *glf-1* worms were incubated with six fluorophore-conjugated plant lectins characterized by different sugar specificities, all of which bound the external surface of *glf-1(RNAi, tm2421, tm2621)* worms, giving rise to distinct patterns of fluorescence (Figs. 4B–G). Staining with WGA and UEA-1 was observed only in the absence of detergent, suggesting that the ligands were solubilized and removed by this treatment. Furthermore, in the presence of detergent, WGA readily penetrated the body cavity of *glf-1* mutants, staining internal structures such as the gonad and the coelomocytes (Fig. 4H). This result indicated an increased permeability of *glf-1* mutants in comparison to WT animals. To explore this possibility further, we stained live *glf-1(tm2412)* mutant larvae with the membrane-impermeable DNA dye Hoechst 33258, used to characterize hyperpermeable mutants. Only 2% of WT larval stages show limited staining with Hoechst 33258 ($n=100$), consistent with previous reports (Moribe et al., 2004), while 100% of *glf-1 (tm2412)* larvae are permeated by the dye ($n=100$; Fig. 4I). Likewise, *glf-1(RNAi, tm2412, tm2621)* worms displayed increased permeability to other dyes, such as trypan blue and SYTO 13, as well hypersensitivity to drugs such as levamisole and ivermectin (data not shown).

glf-1 pattern of expression and subcellular localization of GLF-1::GFP

To determine the expression pattern of *glf-1*, we generated a *glf-1::GFP* translational fusion. This construct fully rescued the Glf-1 phenotype of *tm2412* and *tm2621* animals when carried on an extrachromosomal array; rescue was assessed qualitatively by examining suppression of the Skd phenotype and quantitatively by

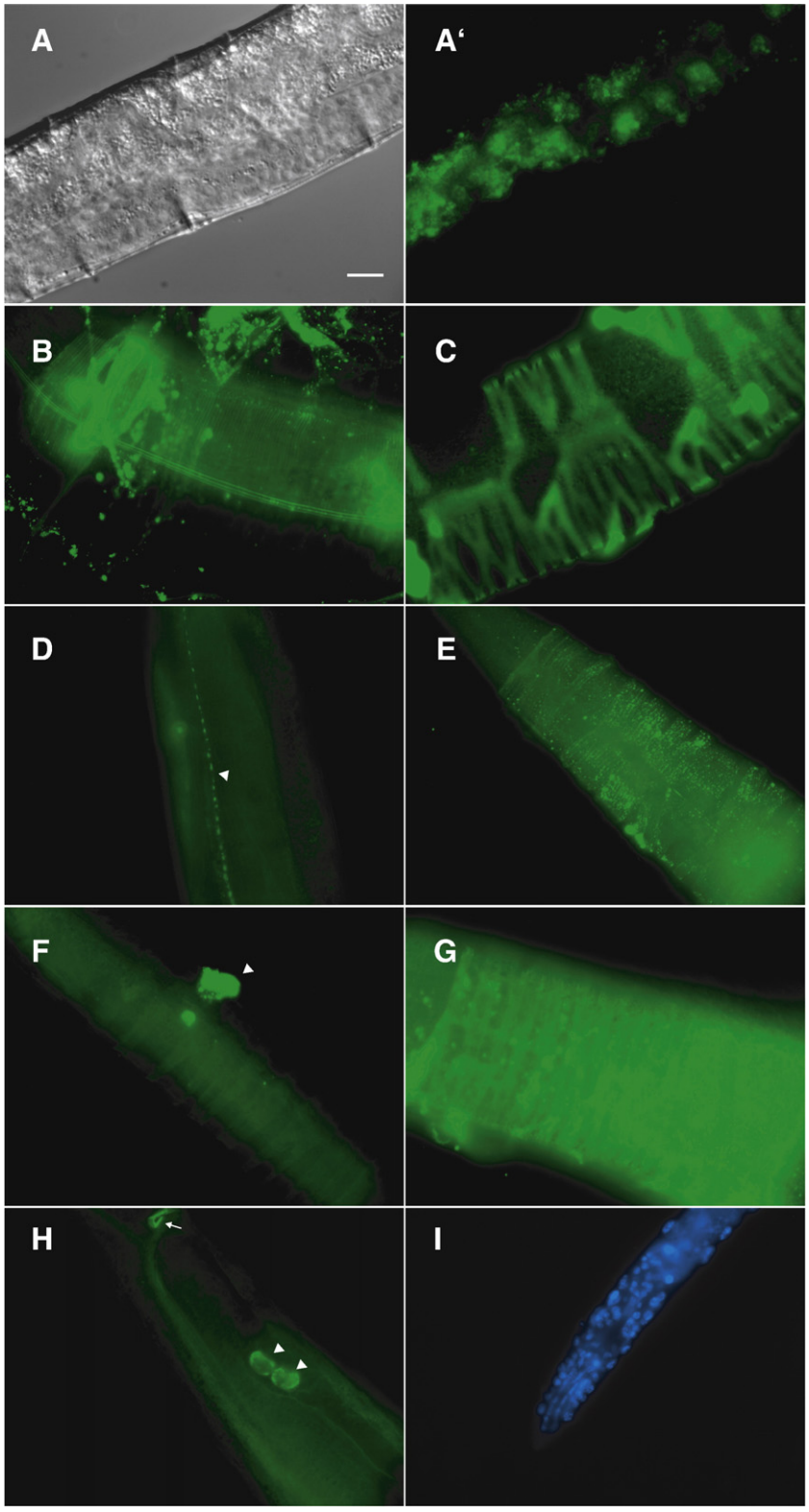

Fig. 4. Lectin and Hoechst 33258 staining of *glf-1* mutants. All lectins used were FITC-conjugated; (A) is a DIC micrograph; the remaining micrographs show exclusively the fluorescence channel. (A and A′) Staining of a WT worm with WGA. No surface binding of WGA can be detected. The fluorescence signal visible represents background fluorescence from the lipid gut granules. Similarly, no labeling of WT worms was detected for the remaining five lectins tested (data not shown). Surface labeling patterns of *glf-1(tm2412)* animals with WGA (B), SBA (C), PEA (D) PSA (E), UEA-1 (F) and ConA (G). Identical patterns of staining were seen in *glf-1(RNAi)* and *glf-1(tm2621)* animals. Incubation of *glf-1* mutants with PSA results in a dimpled staining of the alae (D, white arrowhead), as in other surface-defective mutants (Gravato-Nobre et al., 2005; Yook and Hodgkin, 2007). Note that the antigen recognized by UEA-1 is very loosely bound and forms surface clumps (F, white arrowhead). (H) Penetration of WGA into the pseudocoelomic cavity. Note the staining of the excretory duct (white arrow) and on the surface of two coelomocytes (white arrowheads). (I) Intense Hoechst 33258 staining of a *glf-1(tm2412)* live L2 larva. Scale bar, 20 μm (A).

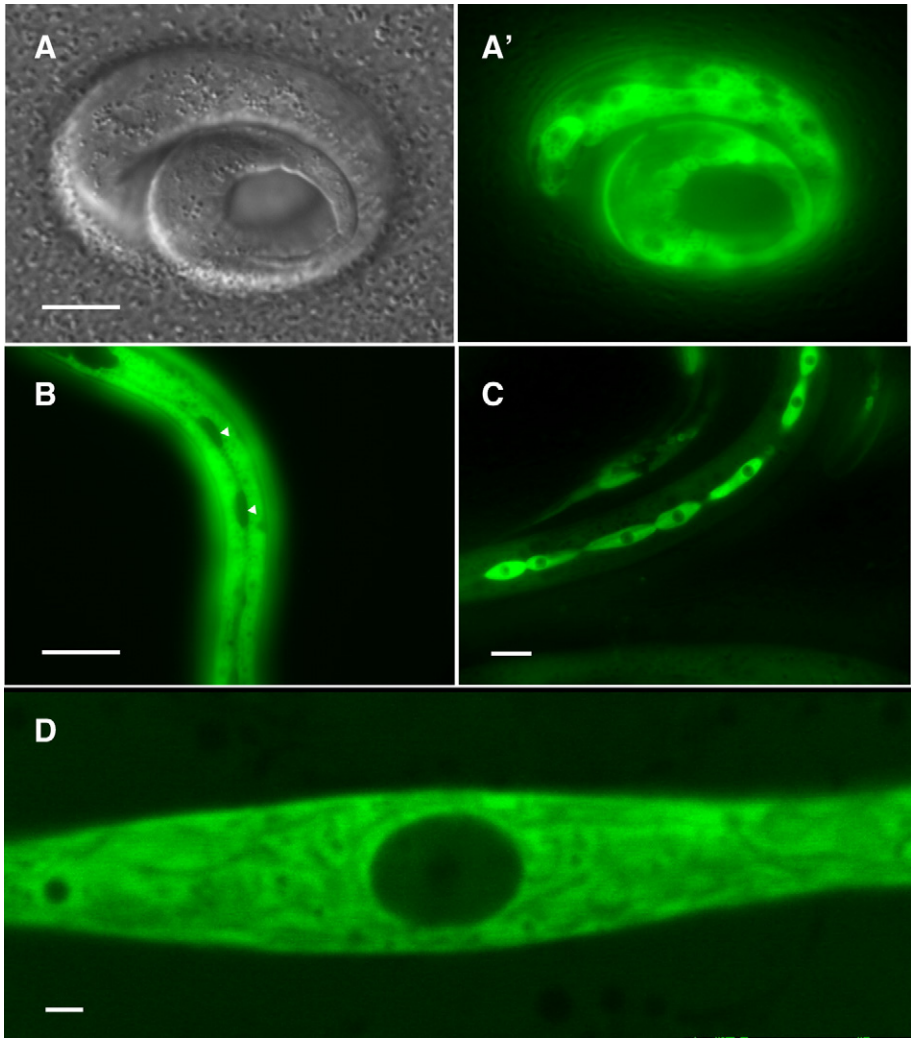

Fig. 5. Expression pattern of *glf-1* and subcellular localization of GLF-1::GFP. Strain IP625 is depicted [genotype: *glf-1(tm2412); osr-1(ok959): nbEx166[glf-1p::Ceglf-1::GFP*]. (A) is the DIC image of (A′). In (B) and (C), only the GFP channel is shown. (D) is a fluorescence confocal micrograph. (A) Four-fold embryo showing the onset of GFP expression. GLF-1::GFP can be seen in the hypodermal cells. (B) Localization of GLF-1::GFP in a L2 larva. The white arrowheads point to two seam cells nuclei. (C) Strong expression of GLF-1::GFP in the seam cells of an L4 larva. (D) Confocal image of a single seam cell of an adult worm expressing the translational fusion. GFP is uniformly distributed within the cytoplasm. Scale bars, 5 μm (A and D) and 20 μm (B and C).

examining the suppression of bleach sensitivity of non-mosaic transgenic animals (Figs. 6A and B). No expression of GLF-1::GFP was seen in early embryogenesis. GFP first became visible at the four-fold embryonic stage, after completion of cuticle synthesis and approximately 1 h before hatching (Figs. 5A and A′). The signal was then seen throughout post-embryonic life. Expression was limited to the hypodermal cells (Figs. 5A–C). L4 larvae and adults showed much stronger expression of GLF-1::GFP in the seam cells as opposed to the main hypodermal syncytium and head and tail hypodermal cells (Fig. 5C). High resolution confocal micrographs of individual seam cells expressing the translational fusion indicate that GLF-1::GFP localizes to the cytoplasm (Fig. 5D).

Transgenic rescue experiments of glf-1 mutants

To confirm that GLF-1 is a functional UGM, we performed a series of transgenic rescue experiments, and quantified the rescue activity of each construct as described above. In addition to the GFP translational fusion described above, full rescue of *glf-1(tm2412)* mutants to WT was obtained with a genomic fragment which included the *glf-1* 5′ UTR, the full *glf-1* genomic region and 2 kb of the *glf-1* 3′ UTR as well as with a fusion of the same promoter sequence to the *C. elegans glf-1* cDNA followed by a 1.9 kb *glf-1* 3′UTR (Fig. 6A). In further tests, we assessed the rescue potential of *E. coli* and *L. major glf*, encoding peptides with proven UGM activity (Beverley et al., 2005; Nassau et al., 1996). The rescue constructs containing the exogenous *glf* genes were arranged like the *C. elegans* cDNA construct (Fig. 6A). While the *E. coli glf* ORF conferred no rescue (data not shown), the *L. major glf* ORF (carried by strains IP614, IP615, IP616, and IP617) alleviated the Glf-1 phenotypes when carried on an extrachromosomal array. The level of sensitivity to bleach in these strains is significantly different from N2 and the mutant (Fig. 6B). This is consistent with the observation that transgenic worms carrying the *L. major glf* construct are also mildly Skd (IP616, Supplementary movie 2). These data indicate that the *L. major glf* ORF is only partially functional and/or poorly expressed in *C. elegans*.

The pathway to Gal$_f$

UDP-Gal$_p$ is the obligate precursor of UDP-Gal$_f$ (Beverley et al., 2005; Nassau et al., 1996; Trejo et al., 1970). UDP-Gal$_p$ is generated by enzymatic conversion of UDP-Glc, catalyzed by the enzyme UDP-Gal 4 epimerase (GalE). *C. elegans* possesses a single GalE homolog, encoded by the *gale-1* ORF (C47B2.6) (Hwang and Horvitz, 2002; Johnston

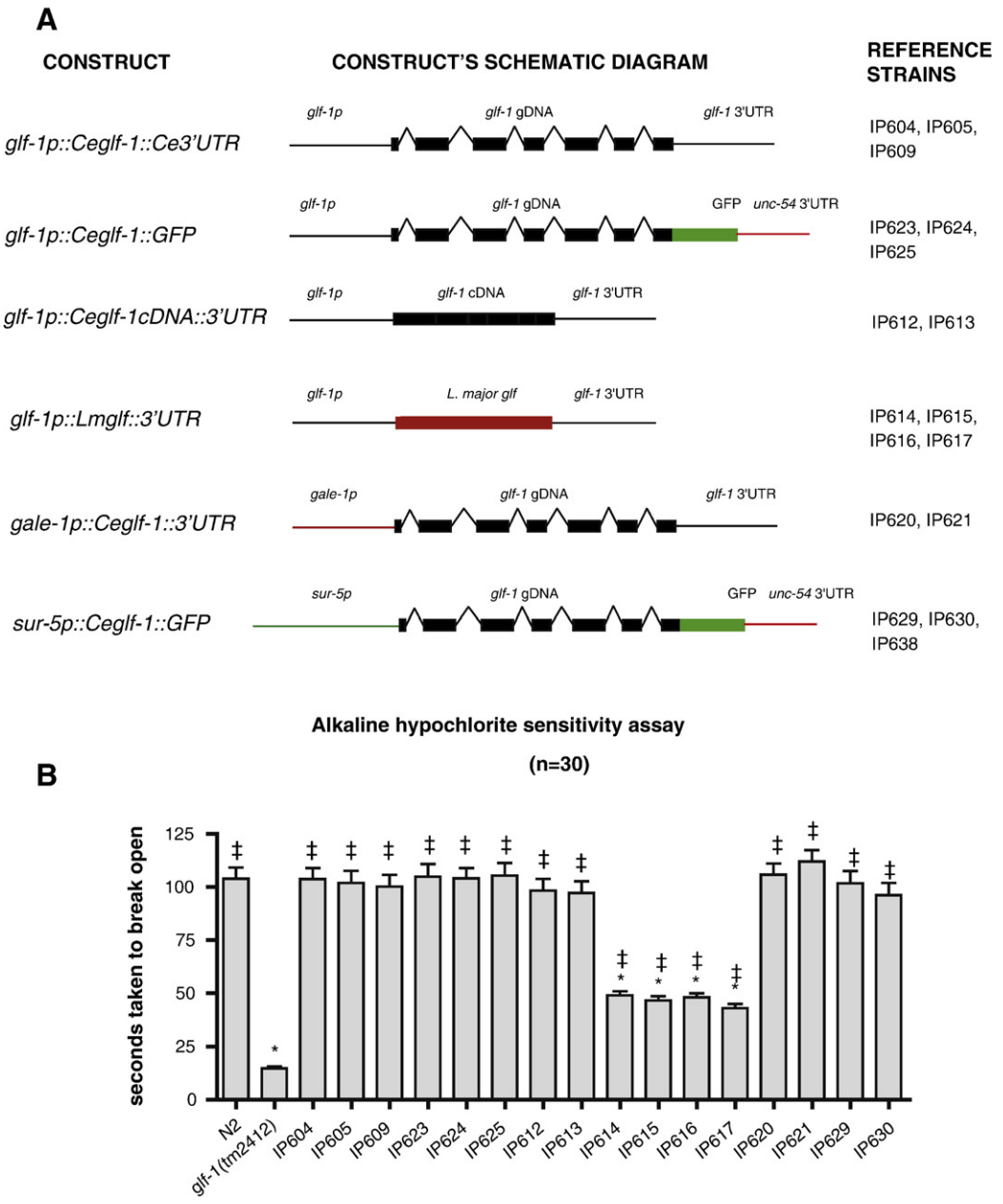

Fig. 6. Transgenic complementation of *glf-1* mutants in an alkaline hypochlorite assay. (A) Diagrammatic representation of the constructs (*Ce* = *C. elegans; Lm* = *L. major*) evaluated and the strains carrying each construct. (B) Alkaline hypochlorite sensitivity assays. The mean and standard error (SEM) values obtained from 30 individual worms are shown. The asterisk indicates those datasets significantly different from N2 in one-way ANOVA significance tests (in all cases $P<0.01$); the double dagger indicates datasets that are significantly different from *glf-1(tm2412)* in one-way ANOVA significance tests (in all cases $P<0.01$).

et al., 2006). We performed RNAi against *gale-1* and found that it faithfully phenocopies the defects seen in *glf-1* mutants but to a lesser extent. *gale-1(RNAi)* worms are mildly Skd and display some lethality (Fig. 3A; $n=844$). In addition, *gale-1(RNAi)* animals display the same range of defects as those observed in *glf-1* mutants, such as superficial blisters, variably placed body constrictions and occurrence of bacterial adherence to the surface (Fig. S2B′). *gale-1* worms are also sensitive to hypochlorite and proteinase K treatment (Figs. 3C–D), and bind a subset of the lectins that stain *glf-1* mutants (Figs. S2A′–C′). We also performed combinatorial *gale-1; glf-1* RNAi. Worms subjected to combined RNAi for these two genes display enhanced Glf-1 phenotypes, which are more severe than those of *glf-1(RNAi)* phenocopies alone (Figs. 3A, C, and D; in Fig. 3A, $n=866$).

To determine whether *glf-1* and *gale-1* are co-expressed, we constructed a *glf-1* genomic construct driven by *gale-1* promoter, which was assayed for transgenic rescue potential. The construct rescued *glf-1* mutants to WT in all stages (Figs. 6A and B), supporting the contention that *gale-1* and *glf-1* expressions overlap throughout the life cycle.

Bacterial adherence and infectivity experiments

M. nematophilum is a pathogen of *Caenorhabditis* nematodes. While not lethal to WT worms, this coryneform, gram-positive bacterium adheres to the post-anal region resulting in a chronic infection (Hodgkin et al., 2000). Since some mutants with defective surface coat structure are not susceptible to *M. nematophilum*, we exposed *glf-1(tm2412)* mutants to *M. nematophilum* and found that the worms died within hours, precluding assessment of infection. We also tested the strain IP616 (Figs. 6A and B), i.e. *glf-1(tm2412)* mutants partially rescued by the *L. major glf* homolog. This strain can be considered equivalent to a *glf-1* reduction-of-function allele, as

judged from the results obtained in the hypochlorite sensitivity assay and the residual Skd phenotype expressed by this strain (Supplementary movie 3). The post-anal region of IP616 worms failed to swell upon challenge with *M. nematophilum* (Figs. 7A and B). Staining with the nucleic acid dye SYTO 13 revealed that *M. nematophilum* cells do not adhere to the post-anal cuticle of IP616 worms (Figs. 7A and B).

NS analysis

To demonstrate the occurrence of Gal_f synthesis in *C. elegans*, we carried out a survey of the nucleotide sugar pools of this organism by adapting a protocol originally devised for analysis of the NS pools of *Trypanosoma* spp. and *L. major* (Turnock and Ferguson, 2007). We extracted and analyzed the NSs of WT worms, *glf-1(tm2412); osr-1 (ok959)* double mutants, and strain IP638 which, besides expressing the endogenous *glf-1* gene, also expresses constitutively and ubiquitously a *glf-1::GFP* reporter. Analysis of WT extracts revealed the presence of all NS precursors for which standards were available, with the exception of GDP-Glc, which is below the level of detection in any *C. elegans* extract analyzed (Fig. 8 and Table 1). In all extracts analyzed, UDP-GlcNAc was the most abundant NS, followed by UDP-Glc; the remaining NSs were present in comparable amounts, with the exception of UDP-Gal_f. In WT animals, UDP-Gal_f was the least abundant of the NSs examined (Fig. 8A). The paucity of this NS precursor precluded its quantitation in WT worms (Table 1). Analysis of *glf-1(tm2412); osr-1(ok959)* double mutants indicated the presence of all NS precursors which we found in WT animals, with the exception of UDP-Gal_f, which could not be detected (Fig. 8B).

We also generated a construct with the *sur-5* promoter, which drives expression of the target gene in most somatic cells beginning in early embryogenesis (Yochem et al., 1998), fused to the *glf-1::GFP* coding sequence (*sur-5p::Ceglf-1::GFP*). Transgenic worms carrying this construct expressed GLF-1::GFP in the cytoplasm of nearly all somatic cells (Fig. S1) from the 300-cell stage onward. Notwithstanding the gross temporal and spatial mis-expression of GLF-1::GFP, this construct rescued *glf-1* mutants to WT (Fig. 6A and B), suggesting that ectopic and early embryonic expression of *glf-1* has no major detrimental effects. The construct was injected into *unc-119(ed3); glf-1(+)* worms together with the *unc-119* rescue plasmid to yield strain IP638. Expression of *glf-1* was measured by semi-quantitative RT-PCR, which showed that in the transgenic strain *glf-1* mRNA is overexpressed approximately 40-fold in comparison to WTs (Fig. S1). Analysis of IP638 worm extracts revealed NS levels comparable to WT animals and *glf-1; osr-1* mutants (Table 1); however, UDP-Gal_f levels were greatly enhanced (Fig. 8C). The increased levels of UDP-Gal_f detected in IP638 worms enabled quantitation of this NS precursor and determination of the UDP-Gal_f/UDP-Gal_p ratio, which is about 1/30 (Table 1).

Discussion

We have investigated the *C. elegans* locus coding for the sole UGM homolog present in this organism, with the aim of determining whether *C. elegans* GLF-1 also functions in the synthesis of Gal_f and if so, what is the importance of this sugar in the biology of the nematode. Our study represents the first comprehensive investigation of a metazoan *glf* gene. The phenotypic characterization of *glf-1* mutants indicate that the gene is essential for viability and that it plays a crucial role in the synthesis of the worm's surface coat. This poorly characterized structure represents the interface between the worm and its environment and acts as a first line of defense against external assault. The phenotypic defects expressed by *glf-1* mutants, such as the traction impairment, superficial blisters and body constrictions, larval lethality, poor long-term survival on plates, surface affinity for plant lectins, occurrence of *E. coli* adherence, hyperpermeability, drug sensitivity and cuticle fragility, have been reported previously for *C. elegans* surface coat mutants (Darby et al., 2007; Gravato-Nobre et al., 2005; Hoflich et al., 2004; Partridge et al., 2008; Yook and Hodgkin, 2007). The swelling of the anal region seen in *glf-1* mutants could also be the result of cuticle fragility. The perianal cuticle is periodically deformed in the defecation cycle, and therefore it could be more prone to become permanently warped in mutants with a compromised cuticle.

A major defect observed in the *glf-1* mutants was the Skd phenotype, which likely arises from loss, depletion or masking of outer cuticle components normally present at the interface between the worm and the substrate on which it moves (Darby et al., 2007). In the plant parasitic nematode *Meloidogyne javanica*, surface-directed antibodies binding to glycocalyx antigens cause a similar kind of traction defect, while at the same time precluding infection of *Arabidopsis thaliana* roots (Sharon et al., 2002).

Surface affinity for plant lectins is an unambiguous indicator of a defect in the synthesis of the glycocalyx; however, no previously described mutant defective in surface coat synthesis stained positive with the whole panel of lectins tested in this work. This is indicative of a significant disruption of surface glyco-conjugates in *glf-1* mutants. The permeability displayed by *glf-1* mutants to WGA was a surprising observation. Normally, harsh procedures such as acetone fixation or collagenase treatment, are required to achieve internal staining of *C. elegans* with lectins (Borgonie et al., 1994). Pseudocoelomic internalization of WGA, which is the smallest of the lectins tested (36 kDa), occurred when the staining buffer was supplemented with 0.1% Triton X-100. This treatment also washed off all the WGA-reactive sugars on the surface. A possible point of entry for WGA is via the compromised surface and/or through excretory pore, as suggested by the observation that the excretory tube stained intensely in *glf-1* animals incubated with WGA (arrow, Fig. 4H).

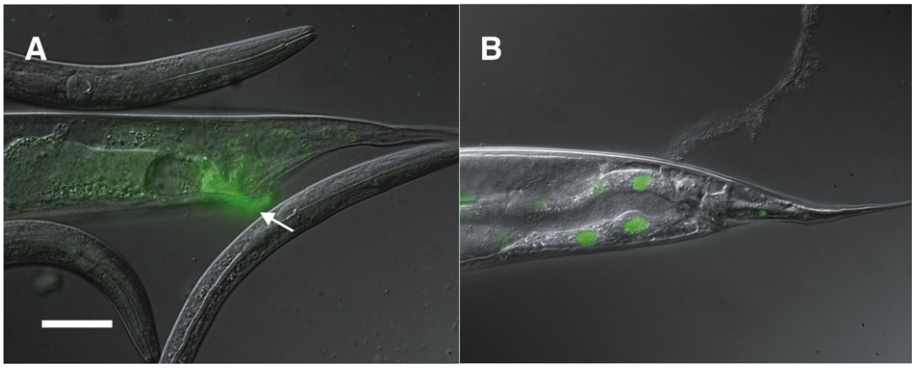

Fig. 7. Challenge of WT and IP616 worms with the pathogenic bacterium *M. nematophilum*. (A) and (B) are dual channel DIC/GFP micrographs. Animals depicted have been stained with the nucleic acid dye SYTO 13 after challenge. (A) A WT worm showing adherence of *M. nematophilum* to the post-anal cuticle and rectal colonization accompanied by swelling of the post-anal region (white arrow). (B) IP616 worm showing the absence of swelling and bacterial adherence to the post-anal region. The green spots visible intracellularly represent nuclear expression of GFP from the *sur-5::GFP* co-injection marker present in this strain. Scale bar, 20 μm (A).

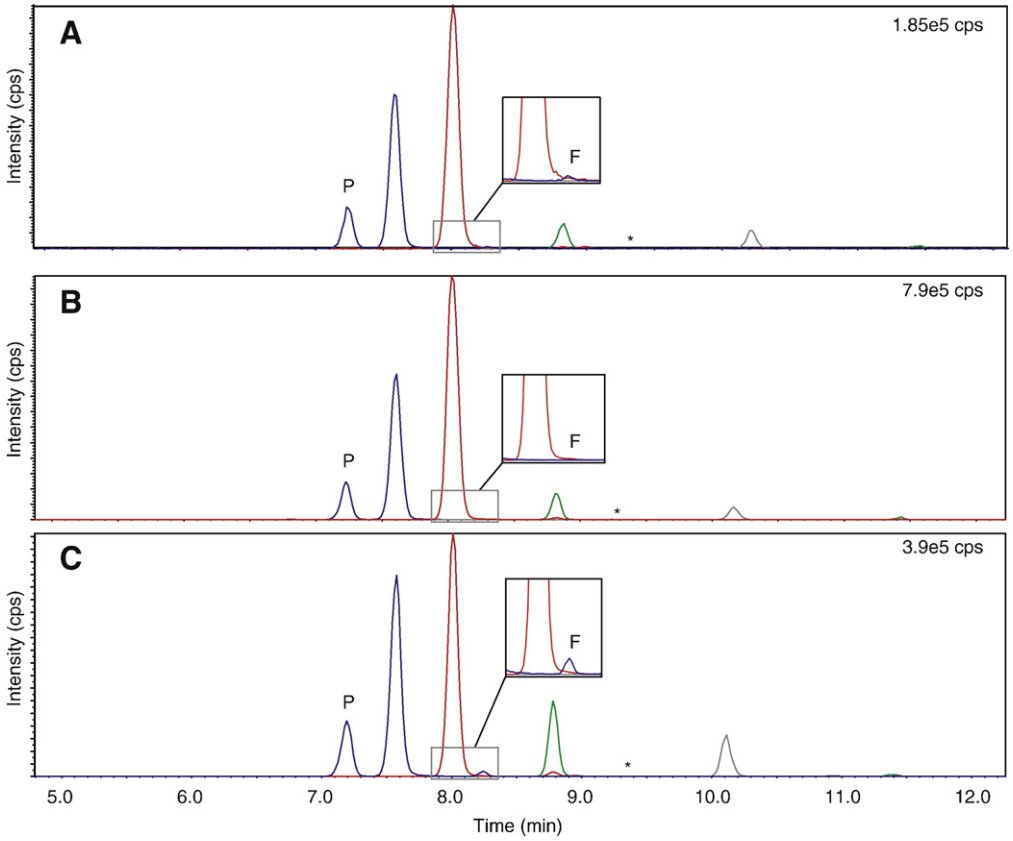

Fig. 8. Electrospray mass spectrometry of sugar nucleotides in WT animals, *glf-1* mutants and IP638 worms. EIC traces were generated at four m/z characteristic of nucleotide sugars. Blue, m/z 564.5–565.5 UDP-Gal$_p$, UDP-Glc, UDP-Gal$_f$; red, m/z 605.5–606.5 UDP-GlcNAc; green, m/z 603.5–604.5 GDP-Man; grey, m/z 587.5–588.5 GDP-Fuc. Intensity was normalized to the most intense sugar nucleotide EIC, UDP-GlcNAc. Insets in each EIC are 300% expansions of the indicated region where UDP-Gal$_f$ was found to elute with an additional 3× expansion in the vertical axis. cps=counts per second. The asterisk marks the expected elution time of GDP-Glc, which was not detected. UDP-Gal$_p$ and UDP-Gal$_f$ are indicated by a P and F, respectively. The three profiles correspond respectively to NS extracts from (A) WT worms, (B) *glf-1(tm2412); osr-1(ok959)* worms and (C) IP638 worms [genotype: *unc-119(ed3); nbEx170 {pDP#MM016b; sur-5p::Ceglf-1::GFP}*].

The pattern of lethality observed in *glf-1* deletion mutants reveals a crucial role for *glf-1* in late embryogenesis. In both cases, more than 89% of the total lethality occurred between the pretzel stage and hatching, and hence after the completion of elongation and cuticle synthesis, suggesting that this may be a direct consequence of a defect in synthesis of the L1 surface coat. Introduction of the *osr-1(ok959)* deletion allele in the *glf-1(tm2412)* background resulted in a remarkable suppression of the lethality (Fig. 3A). The residual lethality was partially shifted to late larval stages, particularly L4s (Fig. 3B). The alleviation of the late embryonic lethality of *glf-1 (tm2412)* mutants by *osr-1* points to constitutive osmotic stress as the main cause of death in late embryos. *osr-1* (which stands for osmotic stress resistance) encodes a novel protein thought to negatively regulate survival in hyperosmotic environments (Solomon et al., 2004). *osr-1* loss-of-function mutants have higher than normal basal levels of glycerol, which results in a specific enhancement of tolerance to osmotic stresses (Solomon et al., 2004). Presumably, in embryos the death occurred upon permeabilization of the eggshell, which causes direct exposure to the external environment without the buffering of the eggshell fluid. The constitutive osmotic stress phenotype is consistent with the increased permeability of *glf-1* mutants and their proneness to desiccation, which has been noticed in other mutants with defective surface coat synthesis (Gravato-Nobre et al., 2005). Interestingly, osmotic stress-related phenotypes are also characteristic of the *Aspergillus* spp. *UGM* mutants (Damveld et al., 2008; El-Ganiny et al., 2008), drawing a direct parallel between homologous gene function in fungi and nematodes.

The spatial and temporal pattern of expression observed for the rescuing GLF-1 translational GFP fusion is in agreement with a role in the formation of the surface coat. GLF-1::GFP is exclusively detected in

Table 1
Quantitative analysis of nucleotide sugar concentration in extracts from three *C. elegans* strains.

	Extracted EIC m/z	Concentration (μM)			NS ratio relative to GlcNAc		
		WT	*glf-1;osr-1*	IP638	WT	*glf-1; osr-1*	IP638
UDP-Gal$_p$	564.5–565.5	3.47 ± 0.20	6.41 ± 0.48	4.46 ± 1.00	0.128	0.138	0.224
UDP-Glc	564.5–565.5	7.63 ± 0.50	13.87 ± 1.74	8.54 ± 2.18	0.279	0.298	0.430
UDP-GlcNAc	605.5–606.5	27.53 ± 1.2	46.51 ± 5.2	19.88 ± 3.35	1.000	1.000	1.000
UDP-Gal$_f$	564.5–565.5	L.O.Q.	N.D.	0.14 ± 0.05	–	–	0.007
GDP-Man	603.5–604.5	3.52 ± 0.20	5.67 ± 0.55	7.14 ± 1.98	0.123	0.122	0.359
GDP-Fuc	587.5–588.5	2.30 ± 0.15	2.96 ± 2.59	4.64 ± 1.12	0.085	0.064	0.233

EICs and integrations were prepared as described in Material and methods. The values are of biological duplicate samples subjected to non-biological triplicate analysis of each duplicate. L.O.Q. = limit of quantitation; N.D. = not detected.

the hypodermal cells, which are responsible for cuticle and surface coat synthesis. Embryonic expression of collagens and collagen processing enzymes involved in synthesis and assembly of the inner layers of the *C. elegans* cuticle occurs in the hypodermal cells starting from the comma or two-fold stages (Johnstone and Barry, 1996; Novelli et al., 2006; Thacker et al., 1995; Winter and Page, 2000). In contrast, GLF-1::GFP is detected at the four-fold stage, after the completion of cuticle synthesis, supporting the hypothesis that GLF-1 is required for formation of the outermost surface layer of the worm, which is presumably the terminal step in the synthesis of the exoskeleton. The enhanced expression of GLF-1::GFP in the seam cells in late larvae and adults is typical of some other genes thought to be involved in synthesis of surface glycans (M. Gravato-Nobre and J. Hodgkin, unpublished results). Therefore seam cells, which have a crucial role in cuticle production and molting (Singh and Sulston, 1978), are also likely key players in orchestrating formation of the glycocalyx.

The cytoplasmic location of the GLF-1::GFP fusion is consistent with a role in NS modification. Eukaryotic UGMs lack signals for secretion or localization to subcellular compartments and are cytoplasmic, similar to their bacterial counterparts (Beverley et al., 2005). The cytoplasmic residency of *L. major* UGM has been demonstrated with a rescuing GFP fusion protein (Kleczka et al., 2007); its ability to partially rescue *glf-1* mutants further confirms that the *C. elegans* GLF-1 is also cytoplasmic.

Our survey of nucleotide sugar pools unequivocally demonstrates the occurrence of synthesis of UDP-Gal$_f$ in *C. elegans* and its absence in *glf-1(tm2412)* mutants, thus confirming the function of the *glf-1* gene as a nematode UGM. UGMs are bidirectional enzymes characterized by equilibrium constants heavily skewed towards UDP-Gal$_p$ production (Nassau et al., 1996; Turnock and Ferguson, 2007). Consistent with this, UDP-Gal$_f$ is a very low abundance nucleotide sugar in WT *C. elegans*, where it can be detected but not quantified at the level of sensitivity attained by our method. Quantification was achieved using a strain (termed IP638) in which *glf-1* is driven constitutively and ubiquitously in most tissues by the *sur-5* promoter. We anticipated higher levels of UDP-Gal$_f$ due to the synthesis and accumulation of the unused precursor in cells where it is normally not produced. Indeed we found approximately a 50-fold increase in the level of *glf-1* expression (Fig. S1), accompanied by increased levels of UDP-Gal$_f$ (Fig. 8C and Table 1). The UDP-Gal$_f$/UDP-Gal$_p$ ratio observed (~3%) in consistent with that observed (~7%) in *E. coli*, *L. major* and *T. cruzi* (Nassau et al., 1996; Turnock and Ferguson, 2007).

Further confirmation that the biosynthetic pathway exists in *C. elegans* was provided by the phenotypic inspection of *gale-1(RNAi)* animals and the synergistic effect of observed in combinatorial RNAi experiments with *glf-1*. In addition, the rescue of *glf-1* mutants by the *C. elegans glf-1* ORF driven by the *gale-1* promoter argues in favor of the hypothesis that *gale-1* and *glf-1* are co-expressed throughout the life cycle.

The finding of UDP-Gal$_f$ raises the question of which nucleotide sugar transporters may be involved in translocation of the precursor into the luminal compartments. *C. elegans* possesses 18 genes coding for nucleotide sugar transporters (reviewed by Berninsone, 2006). However, all the transporters characterized thus far show extensive overlap and redundancy in substrate specificities (Berninsone et al., 2001; Caffaro et al., 2006, 2007, 2008; Hoflich et al., 2004). Based on the similarity of mutant phenotypes expressed, a candidate UDP-Gal$_f$ transporter is SRF-3 (Hoflich et al., 2004). *srf-3* mutants have abnormal surface antigenicity properties (Link et al., 1992), show surface affinity for WGA and SBA (Link et al., 1992), exhibit a mild Skd phenotype and cuticle fragility (Hoflich et al., 2004) and are resistant to infection by *M. nematophilum* (Hodgkin et al., 2000). *srf-3* is required for synthesis of WT levels of Gal-containing glycans (Cipollo et al., 2004) and recombinant SRF-3 can transport UDP-Gal$_p$ and UDP-GlcNAc into *Saccharomyces cerevisiae* Golgi vesicles (Hoflich et al., 2004). However, the pattern of expression of *srf-3* and *glf-1* is only partially overlapping, as judged by the localization of the GFP fusion proteins (Hoflich et al., 2004 and this study), suggesting that there may be additional UDP-Gal$_f$ transporters.

Our results from studies on the IP616 strain implicate *glf-1* and Gal$_f$ residues in infection of *C. elegans* by *M. nematophilum*. IP616 worms, which are *glf-1* mutants partially complemented by the experimentally validated UGM from *L. major*, are resistant to infection because of a lack of pathogen adherence to the worm. Mutants that are resistant to attachment by the bacterium and/or that fail to swell have been isolated and termed *bus* (for bacterially unswollen). Interestingly, some mutants that are resistant to adherence display surface abnormalities similar to *glf-1* mutants. Several *bus* loci characterized by this phenotypic properties have been cloned and found to have mutations in genes encoding components of glycosylation pathways probably because the receptors for attachment of these pathogens are surface glyco-conjugates whose depletion prevents attachment (Gravato-Nobre et al., 2005; Yook and Hodgkin, 2007). Examples are the aforementioned *srf-3*, as well as *bus-8* and *bus-17*, coding for glycosyltransferase homologs and *bus-12*, coding for a sugar nucleotide transporter of unknown specificity (Partridge et al., 2008; Yook and Hodgkin, 2007; M. Gravato-Nobre and J. Hodgkin, unpublished results). It is reasonable to assume that other *bus* genes characterized by the same phenotypic properties as *glf-1* encode the nucleotide sugar transporters and/or galactofuranosyltransferases required for addition of Gal$_f$ to glycan chains. *C. elegans* possesses more than 30 genes coding for predicted galactosyltransferases (reviewed by Berninsone, 2006). Genes encoding galactofuranosyltransferases have been found in *L. major* (Zhang et al., 2004); however, no clear homolog of these transferases nor homologs of the mycobacterial UDP-Gal$_f$-transferases (Belanova et al., 2008; Kremer et al., 2001; Mikusova et al., 2006) nor the putative *E. coli* Gal$_f$-transferase (Wing et al., 2006) is identifiable in the *C. elegans* genome. Identification of the galactofuranosyltransferases and their biochemical characterization will be instrumental in determining the nature of the *C. elegans* glyco-conjugates into which Gal$_f$ residues are incorporated.

The lethality of the *glf-1* mutants upon challenge with *M. nematophilum* appears to conflict with behavior of the IP616 strain and may be mediated by non-specific effects or simply reflect the greatly impaired fitness of these worms. A mutant resistant to attachment of *M. nematophilum* has been reported to be hypersensitive when placed in a different genetic background; in this case the lethality was presumably caused by a non-specific invasion of the body cavity by the pathogenic bacteria (Gravato-Nobre and Hodgkin, 2008).

In light of some of the phenotypes described in *C. elegans glf-1* mutants, namely, enhanced permeability and drug hypersensitivity, studies on UGMs in parasitic nematode species of vertebrates and plants are warranted. Numerous matching ESTs have been identified in parasitic nematodes of humans, animals and plants (Beverley et al., 2005). Should the UGM role be conserved in the phylum, inhibitors of these enzymes, which are currently being developed in other systems, might be used singly or in combination with other treatments to enhance drug permeation. While preliminary attempts to identify UDP-Gal in extracts from the filarial nematode *B. malayi* were unsuccessful (data not shown), there is indirect evidence to support the presence of Gal$_f$ in parasitic nematode species. Intelectins are a family of mammalian lectin-type proteins that bind to Gal$_f$ moieties and Gal$_f$-containing bacterial cell wall preparations (Tsuji et al., 2001). It is thought that intelectins aid in opsonization and recognition of pathogenic bacteria (Tsuji et al., 2001).Transcripts for two intelectins are upregulated in mice during infections of two distantly related parasitic nematodes, *Nippostrongylus brasiliensis* and *T. spiralis* (Pemberton et al., 2004; Voehringer et al., 2007). It is intriguing to speculate that the targets of the mouse intelectins could be Gal$_f$

moieties produced by the pathogenic worms. We are currently determining the chemical nature of Gal_f-containing glyco-conjugates in *C. elegans* using conventional methods and also by isolating *C. elegans* glycans which bind to recombinant intelectins. We would predict the incorporation of Gal_f moieties into surface glycans since this sugar has been exclusively identified in extracellular glyco-conjugates of bacteria, protozoans and fungi, and also given the similarities observed between the mutant *glf* phenotypes seen in *Aspergillus* and *C. elegans.*

Our study did not reveal any novel phenotype associated with a defect in surface coat synthesis; all the phenotypes that we have observed in *glf-1* mutants were described before in other instances. However, our most novel and striking result is the finding that loss of a single sugar is responsible for a series of dramatic phenotypic effects, including hyperpermeability, affinity to lectins, embryonic and larval lethality. Indeed the high levels of lethality displayed by the *glf-1* mutants are interesting and suggest a more critical role of the glycocalyx in development than previously thought. Moreover, we have identified a specific chemical feature and marker for the surface coat, which will facilitate further biochemical and developmental analysis of this poorly characterized but essential structure.

Overall, our results demonstrate the presence of Gal_f in *C. elegans* and reveal its pivotal role in synthesis of the surface coat, a particularly important structure in nematodes, as it represents the interface between the worm and its environment, and likely important for survival of free-living and parasitic species.

Acknowledgments

We gratefully acknowledge the support and encouragement of Dr. Don Comb and the financial support of New England Biolabs. Some nematode strains used in this work were provided by the *Caenorhabditis* Genetics Center (CGC), which is funded by the NIH National Center for Research Resources (NCRR). We wish to thank Dr. Shohei Mitani for additional *C. elegans* strains, Dr. Michael McNeil for the gift of UDP-Gal_f, Drs. Jeremy Foster, Yinhua Zhang, Lisa Maduzia, Zhiru Li and Paul Monaghan for critical reading of the manuscript. We are also thankful to Dr. Paula Magnelli for help with the preparation of NS extracts and to Dr. Maria Gravato-Nobre who performed the *M. nematophilum* challenges and SYTO 13 staining.

Appendix A. Supplementary data

Supplementary data associated with this article can be found, in the online version, at doi:10.1016/j.ydbio.2009.09.010.

References

Ashrafi, K., Chang, F.Y., Watts, J.L., Fraser, A.G., Kamath, R.S., Ahringer, J., Ruvkun, G., 2003. Genome-wide RNAi analysis of *Caenorhabditis elegans* fat regulatory genes. Nature 421, 268–272.

Bakker, H., Kleczka, B., Gerardy-Schahn, R., Routier, F.H., 2005. Identification and partial characterization of two eukaryotic UDP-galactopyranose mutases. Biol. Chem. 386, 657–661.

Beis, K., Srikannathasan, V., Liu, H., Fullerton, S.W., Bamford, V.A., Sanders, D.A., Whitfield, C., McNeil, M.R., Naismith, J.H., 2005. Crystal structures of *Mycobacteria tuberculosis* and *Klebsiella pneumoniae* UDP-galactopyranose mutase in the oxidised state and *Klebsiella pneumoniae* UDP-galactopyranose mutase in the (active) reduced state. J. Mol. Biol. 348, 971–982.

Belanova, M., Dianiskova, P., Brennan, P.J., Completo, G.C., Rose, N.L., Lowary, T.L., Mikusova, K., 2008. Galactosyl transferases in mycobacterial cell wall synthesis. J. Bacteriol. 190, 1141–1145.

Berninsone, P.M., (2006). "Carbohydrates and glycosylation." The *C. elegans* Research Community WormBook, doi:10.1895/wormbook.1.125.1, http://www.wormbook.org.

Berninsone, P., Hwang, H.Y., Zemtseva, I., Horvitz, H.R., Hirschberg, C.B., 2001. SQV-7, a protein involved in *Caenorhabditis elegans* epithelial invagination and early embryogenesis, transports UDP-glucuronic acid, UDP-N-acetylgalactosamine, and UDP-galactose. Proc. Natl. Acad. Sci. U. S. A. 98, 3738–3743.

Beverley, S.M., Owens, K.L., Showalter, M., Griffith, C.L., Doering, T.L., Jones, V.C., McNeil, M.R., 2005. Eukaryotic UDP-galactopyranose mutase (GLF gene) in microbial and metazoal pathogens. Eukaryot Cell 4, 1147–1154.

Bird, A.F., Bird, J., 1991. The Exoskeleton. In: Press, A. (Ed.), The structure of nematodes. San Diego.

Blaxter, M.L., Page, A.P., Rudin, W., Maizels, R.M., 1992. Nematode surface coats: actively evading immunity. Parasitol. Today 8, 243–247.

Borgonie, G., van Driessche, E., Link, C.D., de Waele, D., Coomans, A., 1994. Tissue treatment for whole mount internal lectin staining in the nematodes *Caenorhabditis elegans*, *Panagrolaimus superbus* and *Acrobeloides maximus*. Histochemistry 101, 379–384.

Brenner, S., 1974. The genetics of *Caenorhabditis elegans*. Genetics 77, 71–94.

Caffaro, C.E., Hirschberg, C.B., Berninsone, P.M., 2006. Independent and simultaneous translocation of two substrates by a nucleotide sugar transporter. Proc. Natl. Acad. Sci. U. S. A. 103, 16176–16181.

Caffaro, C.E., Hirschberg, C.B., Berninsone, P.M., 2007. Functional redundancy between two *Caenorhabditis elegans* nucleotide sugar transporters with a novel transport mechanism. J. Biol. Chem. 282, 27970–27975.

Caffaro, C.E., Luhn, K., Bakker, H., Vestweber, D., Samuelson, J., Berninsone, P., Hirschberg, C.B., 2008. A single *Caenorhabditis elegans* Golgi apparatus-type transporter of UDP-glucose, UDP-galactose, UDP-N-acetylglucosamine, and UDP-N-acetylgalactosamine. Biochemistry 47, 4337–4344.

Carlson, E.E., May, J.F., Kiessling, L.L., 2006. Chemical probes of UDP-galactopyranose mutase. Chem. Biol. 13, 825–837.

Chad, J.M., Sarathy, K.P., Gruber, T.D., Addala, E., Kiessling, L.L., Sanders, D.A., 2007. Site-directed mutagenesis of UDP-galactopyranose mutase reveals a critical role for the active-site, conserved arginine residues. Biochemistry 46, 6723–6732.

Cipollo, J.F., Costello, C.E., Hirschberg, C.B., 2002. The fine structure of *Caenorhabditis elegans* N-glycans. J. Biol. Chem. 277, 49143–49157.

Cipollo, J.F., Awad, A.M., Costello, C.E., Hirschberg, C.B., 2004. *srf-3*, a mutant of *Caenorhabditis elegans*, resistant to bacterial infection and to biofilm binding, is deficient in glycoconjugates. J. Biol. Chem. 279, 52893–52903.

Damveld, R.A., Franken, A., Arentshorst, M., Punt, P.J., Klis, F.M., van den Hondel, C.A., Ram, A.F., 2008. A novel screening method for cell wall mutants in *Aspergillus niger* identifies UDP-galactopyranose mutase as an important protein in fungal cell wall biosynthesis. Genetics 178, 873–881.

Darby, C., Chakraborti, A., Politz, S.M., Daniels, C.C., Tan, L., Drace, K., 2007. *Caenorhabditis elegans* mutants resistant to attachment of *Yersinia* biofilms. Genetics 176, 221–230.

De Arruda, M.V., Colli, W., Zingales, B., 1989. Terminal beta-D-galactofuranosyl epitopes recognized by antibodies that inhibit *Trypanosoma cruzi* internalization into mammalian cells. Eur. J. Biochem. 182, 413–421.

de Lederkremer, R.M., Colli, W., 1995. Galactofuranose-containing glycoconjugates in trypanosomatids. Glycobiology 5, 547–552.

Dell, A., Haslam, S.M., Morris, H.R., Khoo, K.H., 1999. Immunogenic glycoconjugates implicated in parasitic nematode diseases. Biochim. Biophys. Acta 1455, 353–362.

Despommier, D.D., Gold, A.M., Buck, S.W., Capo, V., Silberstein, D., 1990. *Trichinella spiralis*: secreted antigen of the infective L1 larva localizes to the cytoplasm and nucleoplasm of infected host cells. Exp. Parasitol. 71, 27–38.

Desvergnes, S., Desvergnes, V., Martin, O.R., Itoh, K., Liu, H.W., Py, S., 2007. Stereoselective synthesis of beta-1-C-substituted 1,4-dideoxy-1,4-imino-D-galactitols and evaluation as UDP-galactopyranose mutase inhibitors. Bioorg. Med. Chem. 15, 6443–6449.

Dykhuizen, E.C., May, J.F., Tongpenyai, A., Kiessling, L.L., 2008. Inhibitors of UDP-galactopyranose mutase thwart mycobacterial growth. J. Am. Chem. Soc. 130, 6706–6707.

El-Ganiny, A.M., Sanders, D.A., Kaminskyj, S.G., 2008. *Aspergillus nidulans* UDP-galactopyranose mutase, encoded by ugmA plays key roles in colony growth, hyphal morphogensis, and conidiation. Fungal Genet. Biol. 45, 1533–1542.

Fire, A., Xu, S., Montgomery, M.K., Kostas, S.A., Driver, S.E., Mello, C.C., 1998. Potent and specific genetic interference by double-stranded RNA in *Caenorhabditis elegans*. Nature 391, 806–811.

Ghavami, A., Chen, J.J., Mario Pinto, B., 2004. Synthesis of a novel class of sulfonium ions as potential inhibitors of UDP-galactopyranose mutase. Carbohydr. Res. 339, 401–407.

Gravato-Nobre, M.J., Hodgkin, J., 2008. The acyltransferase gene *bus-1* exhibits conserved and specific expression in nematode rectal cells and reveals pathogen-induced cell swelling. Dev. Dyn. 237, 3762–3776.

Gravato-Nobre, M.J., Nicholas, H.R., Nijland, R., O'Rourke, D., Whittington, D.E., Yook, K.J., Hodgkin, J., 2005. Multiple genes affect sensitivity of *Caenorhabditis elegans* to the bacterial pathogen *Microbacterium nematophilum*. Genetics 171, 1033–1045.

Guerardel, Y., Balanzino, L., Maes, E., Leroy, Y., Coddeville, B., Oriol, R., Strecker, G., 2001. The nematode *Caenorhabditis elegans* synthesizes unusual O-linked glycans: identification of glucose-substituted mucin-type O-glycans and short chondroitin-like oligosaccharides. Biochem. J. 357, 167–182.

Harnett, W., Harnett, M.M., 2001. Modulation of the host immune system by phosphorylcholine-containing glycoproteins secreted by parasitic filarial nematodes. Biochim. Biophys. Acta 1539, 7–15.

Hearn, V.M., Griffiths, B.L., Gorin, P.A., 1989. Structural analysis of water-soluble fractions obtained from *Aspergillus fumigatus* mycelium. Glycoconj. J. 6, 85–100.

Hodgkin, J., Kuwabara, P.E., Corneliussen, B., 2000. A novel bacterial pathogen, *Microbacterium nematophilum*, induces morphological change in the nematode *C. elegans*. Curr. Biol. 10, 1615–1618.

Hoflich, J., Berninsone, P., Gobel, C., Gravato-Nobre, M.J., Libby, B.J., Darby, C., Politz, S. M., Hodgkin, J., Hirschberg, C.B., Baumeister, R., 2004. Loss of *srf-3*-encoded

nucleotide sugar transporter activity in *Caenorhabditis elegans* alters surface antigenicity and prevents bacterial adherence. J. Biol. Chem. 279, 30440–30448.
Hwang, H.Y., Horvitz, H.R., 2002. The SQV-1 UDP-glucuronic acid decarboxylase and the SQV-7 nucleotide-sugar transporter may act in the Golgi apparatus to affect *Caenorhabditis elegans* vulval morphogenesis and embryonic development. Proc. Natl. Acad. Sci. U. S. A. 99, 14218–14223.
Ilg, T., Etges, R., Overath, P., McConville, M.J., Thomas-Oates, J., Thomas, J., Homans, S.W., Ferguson, M.A., 1992. Structure of *Leishmania mexicana* lipophosphoglycan. J. Biol. Chem. 267, 6834–6840.
Itoh, K., Huang, Z., Liu, H.W., 2007. Synthesis and analysis of substrate analogues for UDP-galactopyranose mutase: implication for an oxocarbenium ion intermediate in the catalytic mechanism. Org. Lett. 9, 879–882.
James, P.G., Cherniak, R., 1992. Galactoxylomannans of *Cryptococcus neoformans*. Infect. Immun. 60, 1084–1088.
Johnston, W.L., Krizus, A., Dennis, J.W., 2006. The eggshell is required for meiotic fidelity, polar-body extrusion and polarization of the *C. elegans* embryo. BMC Biol. 4, 35.
Johnstone, I.L., Barry, J.D., 1996. Temporal reiteration of a precise gene expression pattern during nematode development. EMBO J. 15, 3633–3639.
Kamath, R.S., Fraser, A.G., Dong, Y., Poulin, G., Durbin, R., Gotta, M., Kanapin, A., Le Bot, N., Moreno, S., Sohrmann, M., Welchman, D.P., Zipperlen, P., Ahringer, J., 2003. Systematic functional analysis of the *Caenorhabditis elegans* genome using RNAi. Nature 421, 231–237.
Khoo, K.H., Maizels, R.M., Page, A.P., Taylor, G.W., Rendell, N.B., Dell, A., 1991. Characterization of nematode glycoproteins: the major O-glycans of *Toxocara* excretory-secretory antigens are O-methylated trisaccharides. Glycobiology 1, 163–171.
Kleczka, B., Lamerz, A.C., van Zandbergen, G., Wenzel, A., Gerardy-Schahn, R., Wiese, M., Routier, F.H., 2007. Targeted gene deletion of *Leishmania major* UDP-galactopyranose mutase leads to attenuated virulence. J. Biol. Chem. 282, 10498–10505.
Koplin, R., Brisson, J.R., Whitfield, C., 1997. UDP-galactofuranose precursor required for formation of the lipopolysaccharide O antigen of *Klebsiella pneumoniae* serotype O1 is synthesized by the product of the rfbDKPO1 gene. J. Biol. Chem. 272, 4121–4128.
Kremer, L., Dover, L.G., Morehouse, C., Hitchin, P., Everett, M., Morris, H.R., Dell, A., Brennan, P.J., McNeil, M.R., Flaherty, C., Duncan, K., Besra, G.S., 2001. Galactan biosynthesis in *Mycobacterium tuberculosis*. Identification of a bifunctional UDP-galactofuranosyltransferase. J. Biol. Chem. 276, 26430–26440.
Link, C.D., Silverman, M.A., Breen, M., Watt, K.E., Dames, S.A., 1992. Characterization of *Caenorhabditis elegans* lectin-binding mutants. Genetics 131, 867–881.
Maduro, M., Pilgrim, D., 1995. Identification and cloning of *unc-119*, a gene expressed in the *Caenorhabditis elegans* nervous system. Genetics 141, 977–988.
Maizels, R.M., Kennedy, M.W., Meghji, M., Robertson, B.D., Smith, H.V., 1987. Shared carbohydrate epitopes on distinct surface and secreted antigens of the parasitic nematode *Toxocara canis*. J. Immunol. 139, 207–214.
McConville, M.J., Homans, S.W., Thomas-Oates, J.E., Dell, A., Bacic, A., 1990. Structures of the glycoinositolphospholipids from *Leishmania major*. A family of novel galactofuranose-containing glycolipids. J. Biol. Chem. 265, 7385–7394.
McVay, C.S., Tsung, A., Appleton, J., 1998. Participation of parasite surface glycoproteins in antibody-mediated protection of epithelial cells against *Trichinella spiralis*. Infect. Immun. 66, 1941–1945.
Mello, C.C., Kramer, J.M., Stinchcomb, D., Ambros, V., 1991. Efficient gene transfer in *C. elegans*: extrachromosomal maintenance and integration of transforming sequences. EMBO J. 10, 3959–3970.
Mikusova, K., Belanova, M., Kordulakova, J., Honda, K., McNeil, M.R., Mahapatra, S., Crick, D.C., Brennan, P.J., 2006. Identification of a novel galactosyl transferase involved in biosynthesis of the mycobacterial cell wall. J. Bacteriol. 188, 6592–6598.
Moribe, H., Yochem, J., Yamada, H., Tabuse, Y., Fujimoto, T., Mekada, E., 2004. Tetraspanin protein (TSP-15) is required for epidermal integrity in *Caenorhabditis elegans*. J. Cell. Sci. 117, 5209–5220.
Nassau, P.M., Martin, S.L., Brown, R.E., Weston, A., Monsey, D., McNeil, M.R., Duncan, K., 1996. Galactofuranose biosynthesis in *Escherichia coli* K-12: identification and cloning of UDP-galactopyranose mutase. J. Bacteriol. 178, 1047–1052.
Nielsen, K., Heitman, J., 2007. Sex and virulence of human pathogenic fungi. Adv. Genet. 57, 143–173.
Novelli, J., Page, A.P., Hodgkin, J., 2006. The C terminus of collagen SQT-3 has complex and essential functions in nematode collagen assembly. Genetics 172, 2253–2267.
Page, A.P., and Johnstone, I.L., (2007). The cuticle. In "Wormbook doi/10.1895/wormbook.1.7.1, http://www.wormbook.org." (T. C. e. r. community, Ed.
Page, A.P., Rudin, W., Fluri, E., Blaxter, M.L., Maizels, R.M., 1992. *Toxocara canis*: a labile antigenic surface coat overlying the epicuticle of infective larvae. Exp. Parasitol. 75, 72–86.
Pan, F., Jackson, M., Ma, Y., McNeil, M., 2001. Cell wall core galactofuran synthesis is essential for growth of mycobacteria. J. Bacteriol. 183, 3991–3998.
Partridge, F.A., Tearle, A.W., Gravato-Nobre, M.J., Schafer, W.R., Hodgkin, J., 2008. The *C. elegans* glycosyltransferase BUS-8 has two distinct and essential roles in epidermal morphogenesis. Dev. Biol. 317, 549–559.
Pedersen, L.L., Turco, S.J., 2003. Galactofuranose metabolism: a potential target for antimicrobial chemotherapy. Cell. Mol. Life Sci. 60, 259–266.
Pemberton, A.D., Knight, P.A., Gamble, J., Colledge, W.H., Lee, J.K., Pierce, M., Miller, H.R., 2004. Innate BALB/c enteric epithelial responses to *Trichinella spiralis*: inducible expression of a novel goblet cell lectin, intelectin-2, and its natural deletion in C57BL/10 mice. J. Immunol. 173, 1894–1901.
Plackett, P., Buttery, S.H., 1964. A galactofuranose disaccharide from the galactan of *Mycoplasma mycoides*. Biochem. J. 90, 201–205.
Poirot, O., O'Toole, E., Notredame, C., 2003. Tcoffee@igs: a web server for computing, evaluating and combining multiple sequence alignments. Nucleic Acids Res. 31, 3503–3506.
Previato, J.O., Gorin, P.A., Mazurek, M., Xavier, M.T., Fournet, B., Wieruszesk, J.M., Mendonca-Previato, L., 1990. Primary structure of the oligosaccharide chain of lipopeptidophosphoglycan of epimastigote forms of *Trypanosoma cruzi*. J. Biol. Chem. 265, 2518–2526.
Rabina, J., Maki, M., Savilahti, E.M., Jarvinen, N., Penttila, L., Renkonen, R., 2001. Analysis of nucleotide sugars from cell lysates by ion-pair solid-phase extraction and reversed-phase high-performance liquid chromatography. Glycoconj. J. 18, 799–805.
Rual, J.F., Ceron, J., Koreth, J., Hao, T., Nicot, A.S., Hirozane-Kishikawa, T., Vandenhaute, J., Orkin, S.H., Hill, D.E., van den Heuvel, S., Vidal, M., 2004. Toward improving *Caenorhabditis elegans* phenome mapping with an ORFeome-based RNAi library. Genome Res. 14, 2162–2168.
Sambrook, J., Fritsch, E.F., Maniatis, T., 1989. Molecular cloning. A laboratory manual. Second edition. Cold Spring harbor laboratory press.
Samuelson, A.V., Carr, C.E., Ruvkun, G., 2007. Gene activities that mediate increased life span of *C. elegans* insulin-like signaling mutants. Genes Dev. 21, 2976–2994.
Sanders, D.A., Staines, A.G., McMahon, S.A., McNeil, M.R., Whitfield, C., Naismith, J.H., 2001. UDP-galactopyranose mutase has a novel structure and mechanism. Nat. Struct. Biol. 8, 858–863.
Sarvas, M., Nikaido, H., 1971. Biosynthesis of T1 antigen in *Salmonella*: origin of D-galactofuranose and D-ribofuranose residues. J. Bacteriol. 105, 1063–1072.
Schabussova, I., Amer, H., van Die, I., Kosma, P., Maizels, R.M., 2007. O-methylated glycans from *Toxocara* are specific targets for antibody binding in human and animal infections. Int. J. Parasitol. 37, 97–109.
Scherman, M.S., Winans, K.A., Stern, R.J., Jones, V., Bertozzi, C.R., McNeil, M.R., 2003. Drug targeting *Mycobacterium tuberculosis* cell wall synthesis: development of a microtiter plate-based screen for UDP-galactopyranose mutase and identification of an inhibitor from a uridine-based library. Antimicrob. Agents Chemother. 47, 378–382.
Schmalhorst, P.S., Krappmann, S., Vervecken, W., Rohde, M., Muller, M., Braus, G.H., Contreras, R., Braun, A., Bakker, H., Routier, F.H., 2008. Contribution of galactofuranose to the virulence of the opportunistic pathogen *Aspergillus fumigatus*. Eukaryotic Cell 7, 1268–1277.
Sharon, E., Spiegel, Y., Salomon, R., Curtis, R.H., 2002. Characterization of *Meloidogyne javanica* surface coat with antibodies and their effect on nematode behaviour. Parasitology 125, 177–185.
Silverman, M.A., Blaxter, M.L., Link, C.D., 1997. Biochemical analysis of *Caenorhabditis elegans* surface mutants. J. Nematol. 29, 296–305.
Simmer, F., Moorman, C., van der Linden, A.M., Kuijk, E., van den Berghe, P.V., Kamath, R.S., Fraser, A.G., Ahringer, J., Plasterk, R.H., 2003. Genome-wide RNAi of *C. elegans* using the hypersensitive *rrf-3* strain reveals novel gene functions. PLoS Biol. 1, E12.
Singh, R.N., Sulston, J.E., 1978. Some observations on molting in *C. elegans*. Nematologica 24.
Solomon, A., Bandhakavi, S., Jabbar, S., Shah, R., Beitel, G.J., Morimoto, R.I., 2004. *Caenorhabditis elegans* OSR-1 regulates behavioral and physiological responses to hyperosmotic environments. Genetics 167, 161–170.
Soltero-Higgin, M., Carlson, E.E., Phillips, J.H., Kiessling, L.L., 2004. Identification of inhibitors for UDP-galactopyranose mutase. J. Am. Chem. Soc. 126, 10532–10533.
Spath, G.F., Garraway, L.A., Turco, S.J., Beverley, S.M., 2003. The role(s) of lipophosphoglycan (LPG) in the establishment of *Leishmania major* infections in mammalian hosts. Proc. Natl. Acad. Sci. U. S. A. 100, 9536–9541.
Stevenson, G., Neal, B., Liu, D., Hobbs, M., Packer, N.H., Batley, M., Redmond, J.W., Lindquist, L., Reeves, P., 1994. Structure of the O antigen of *Escherichia coli* K-12 and the sequence of its rfb gene cluster. J. Bacteriol. 176, 4144–4156.
Sulston, J.E., Hodgkin, J.A., 1988. Methods. In: Press, C.S.H.L. (Ed.), The nematode *Caenorhabditis elegans*, pp. 587–606.
Thacker, C., Peters, K., Srayko, M., Rose, A.M., 1995. The bli-4 locus of *Caenorhabditis elegans* encodes structurally distinct kex2/subtilisin-like endoproteases essential for early development and adult morphology. Genes Dev. 9, 956–971.
Trejo, A.G., Chittenden, G.J., Buchanan, J.G., Baddiley, J., 1970. Uridine diphosphate alpha-D-galactofuranose, an intermediate in the biosynthesis of galactofuranosyl residues. Biochem. J. 117, 637–639.
Tsuji, S., Uehori, J., Matsumoto, M., Suzuki, Y., Matsuhisa, A., Toyoshima, K., Seya, T., 2001. Human intelectin is a novel soluble lectin that recognizes galactofuranose in carbohydrate chains of bacterial cell wall. J. Biol. Chem. 276, 23456–23463.
Turco, S.J., Orlandi Jr., P.A., Homans, S.W., Ferguson, M.A., Dwek, R.A., Rademacher, T.W., 1989. Structure of the phosphosaccharide-inositol core of the Leishmania donovani lipophosphoglycan. J. Biol. Chem. 264, 6711–6715.
Turnock, D.C., Ferguson, M.A., 2007. The sugar nucleotide pools of *Trypanosoma brucei*, *Trypanosoma cruzi* and *Leishmania major*. Eukaryot Cell 6, 1450–1463.
Varki, A., 1993. Biological roles of oligosaccharides: all of the theories are correct. Glycobiology 3, 97–130.
Veerapen, N., Yuan, Y., Sanders, D.A., Pinto, B.M., 2004. Synthesis of novel ammonium and selenonium ions and their evaluation as inhibitors of UDP-galactopyranose mutase. Carbohydr. Res. 339, 2205–2217.
Voehringer, D., Stanley, S.A., Cox, J.S., Completo, G.C., Lowary, T.L., Locksley, R.M., 2007. *Nippostrongylus brasiliensis*: identification of intelectin-1 and -2 as Stat6-dependent genes expressed in lung and intestine during infection. Exp. Parasitol. 116, 458–466.
Wallis, G.L., Hemming, F.W., Peberdy, J.F., 2001. Beta-galactofuranoside glycoconjugates on conidia and conidiophores of *Aspergillus niger*. FEMS Microbiol. Lett. 201, 21–27.

Weston, A., Stern, R.J., Lee, R.E., Nassau, P.M., Monsey, D., Martin, S.L., Scherman, M.S., Besra, G.S., Duncan, K., McNeil, M.R., 1997. Biosynthetic origin of mycobacterial cell wall galactofuranosyl residues. Tuber. Lung Dis. 78, 123–131.

Wing, C., Errey, J.C., Mukhopadhyay, B., Blanchard, J.S., Field, R.A., 2006. Expression and initial characterization of WbbI, a putative D-Galf:alpha-D-Glc beta-1,6-galactofuranosyltransferase from *Escherichia coli* K-12. Org. Biomol. Chem. 4, 3945–3950.

Winter, A.D., Page, A.P., 2000. Prolyl 4-hydroxylase is an essential procollagen-modifying enzyme required for exoskeleton formation and the maintenance of body shape in the nematode *Caenorhabditis elegans*. Mol. Cell. Biol. 20, 4084–4093.

Wisnewski, N., McNeil, M., Grieve, R.B., Wassom, D.L., 1993. Characterization of novel fucosyl- and tyvelosyl-containing glycoconjugates from *Trichinella spiralis* muscle stage larvae. Mol. Biochem. Parasitol. 61, 25–35.

Yochem, J., Gu, T., Han, M., 1998. A new marker for mosaic analysis in *Caenorhabditis elegans* indicates a fusion between hyp6 and hyp7, two major components of the hypodermis. Genetics 149, 1323–1334.

Yook, K., Hodgkin, J., 2007. Mos1 mutagenesis reveals a diversity of mechanisms affecting response of *Caenorhabditis elegans* to the bacterial pathogen *Microbacterium nematophilum*. Genetics 175, 681–697.

Zhang, K., Barron, T., Turco, S.J., Beverley, S.M., 2004. The LPG1 gene family of *Leishmania major*. Mol. Biochem. Parasitol. 136, 11–23.